Field performance of the cardenolide-producing crucifer *Erysimum cheiranthoides* under herbivore attack and heterospecific competition

Kunqi Wang[1], Erik van Bergen[1,2] and Tobias Züst[1]

[1]Institute of Systematic and Evolutionary Botany, University of Zürich, Zollikerstrasse 107, CH-8008 Zürich

[2] CE3C - Centre for Ecology, Evolution and Environmental Changes & CHANGE – Global Change and Sustainability Institute, Faculty of Sciences, University of Lisbon (FCUL), 1749-016 Lisbon, Portugal

Corresponding author: Tobias Züst *(tobias.zuest@systbot.uzh.ch)*

Abstract

1. Plants in the Brassicaceae produce glucosinolates as potent defences against generalist herbivores, but many specialists have evolved the ability to tolerate or even deactivate these compounds. As a possible co-evolutionary response to attack by specialists, plants in the genus *Erysimum* gained the ability to produce novel cardenolide defences in addition to ancestral glucosinolates.
2. We grew the dually defended *E. cheiranthoides* side-by-side with the phenologically similar *Rhamnospermum nigrum* (syn. *Brassica nigra*) in agricultural fields surrounded by other Brassicaceae crops. Over the course of two field seasons, we monitored focal plants to characterise their associated herbivore community, and we quantified herbivore damage and measured plant growth. In the second year, we additionally manipulated herbivore density and plant competition to identify direct and indirect effects on plant fitness.
3. Both plant species were attacked by a diverse community of specialist herbivores already present on the surrounding Brassicaceae crops. Most herbivores strongly favoured *R. nigrum*, reaching higher densities and causing intense damage that largely suppressed growth of these plants. A similar community of herbivores attacked *E. cheiranthoides*, but at much lower densities that caused little damage and did not impact plant growth.
4. In accordance with differential susceptibilities to herbivores, herbivore removal benefitted *R. nigrum* by reducing damage and increasing plant growth, while it had no positive effect on *E. cheiranthoides*. In fact, herbivore removal had an indirect negative effect on *E. cheiranthoides* plants growing in conspecific pairs, as they suffered from increased competition by otherwise herbivore-suppressed *R. nigrum*.
5. Our results agree with a successful escape of *E. cheiranthoides* from herbivory, as even though plants are still attacked when herbivores are abundant, these herbivores cause little damage and cause no reduction in fitness. However, the escape from herbivory has likely come at loss of competitive ability when herbivore pressure is low, which would explain why

despite its key innovation, *E. cheiranthoides* has been unable to gain dominance in any plant community.

Keywords: Enemy-free space, chemical novelty, plant defence, herbivore-imposed selection

1. Introduction

In nature, plants are constantly threatened by herbivores that consume a substantial proportion of global plant biomass and cause major yield losses in agriculture (Johnson, 2011). To protect their limited resources, plants have evolved multiple layers of defence, including physical barriers and a vast array of chemical compounds (War et al., 2012). Chemical defences play a particularly important role in plant-herbivore interactions, as they shape herbivore community composition, and are themselves shaped by herbivore-imposed selection (Agrawal, Hastings, et al., 2012; Züst et al., 2012). Over evolutionary time, reciprocal adaptations between plants and herbivores have produced a remarkable diversity of toxic, repellent, or antinutritive compounds across plant lineages (Speed et al., 2015).

Plant resistance traits such as chemical defences require significant energetic and metabolic investment. For example, glucosinolate production in Brassicaceae species can consume up to 15% of a plant's total photosynthetic energy (Bekaert et al., 2012). Defence traits therefore represent major costs for plants, both directly through reduced allocation to other functions (direct or allocation costs, Herms & Mattson, 1992; Züst & Agrawal, 2017) and indirectly by altering interactions with mutualists or competitors (ecological costs, Strauss et al., 2002). Importantly, both costs and benefits of defence depend on the environmental context. According to the growth-differentiation balance (GDH) hypothesis, plants face a physiological trade-off between rapid growth and strong defence (Herms & Mattson, 1992), yet rapid growth is most advantageous during establishment in competitive environments (Züst et al., 2011), while costs may be lower under different conditions. Similarly, high defence investments should be favoured only when herbivory is intense and when herbivores are susceptible to that defence (Simms & Rausher, 1987).

The interplay between competition, defence, and herbivory has been repeatedly demonstrated in experimental systems (Hambäck & Beckerman, 2003). Manipulating herbivore pressure often leads to striking shifts in defence expression and plant-plant competition (Mauricio & Rausher, 1997; Züst et al., 2012). Interestingly, the natural gains of novel defences can mirror the effects of experimental herbivore exclusion: the acquisition of a potent new defence may allow plants to temporarily escape herbivore-imposed selection, thereby altering competitive dynamics and facilitating colonization of new habitats ("escape and radiate", Ehrlich & Raven, 1964).

A classic example of escape-and-radiate comes from the order Brassicales, in which the evolution of glucosinolate defences approximately 80 million years ago triggered rapid species diversification (Edger et al., 2015). Over evolutionary time, specialist herbivores evolved counteradaptations that allow them to tolerate or even exploit these defences (Ratzka et al., 2002; Sporer et al., 2021; Wittstock et al., 2004). As a result, most extant species of the Brassicaceae are attacked by diverse communities of glucosinolate-resistant herbivores (Bidart-Bouzat & Kliebenstein, 2008; Mertens et al., 2021). However, despite the limited effectiveness of glucosinolates against these specialists, Brassicaceae species still produce a wide variety of these compounds (Fahey et al., 2001), highlighting the challenges of inferring early selective pressures that shaped defence evolution from present-day interactions.

Because long-term coevolution can obscure the processes that initially selected for new resistance traits, focusing on defences of recent evolutionary origin provides a valuable opportunity to study costs and benefits before specialized antagonists evolve. In one such example, species of the genus *Erysimum* (Brassicaceae) evolved the ability to synthesize cardenolide toxins within the last five million years (Züst et al., 2020). Cardenolides are a potent inhibitors of animal Na^+/K^+-ATPases, thus their mode of action differs fundamentally from that of glucosinolates (Agrawal, Petschenka, et al., 2012). Consequently, some glucosinolate-resistant herbivores are completely repelled by *Erysimum* plants (Sachdev-Gupta et al., 1993; Younkin et al., 2024; but see Wang & Züst, 2025). This apparent 'escape' from herbivores may have enable a recent radiation within this diverse genus (Züst et al., 2020). Most *Erysimum* species co-express both glucosinolate and cardenolide defences, but while interspecific variation in glucosinolates is limited, cardenolide profiles are highly variable (Züst

et al., 2020), potentially reflecting differential selection on the novel defence. To date, no herbivore has evolved specialised resistance to *Erysimum* cardenolides, and only one cardenolide-specialised seed bug has expanded its host range to include *Erysimum* (Petschenka et al., 2022). This system therefore offers a rare opportunity to examine the ecological consequences of a newly evolved defence before coevolution reshapes the interaction.

Here, we use the annual *Erysimum cheiranthoides* to characterise the natural herbivore community attacking this species in central Europe. Specifically, we ask whether the evolution of cardenolide production has allowed *E. cheiranthoides* to escape from herbivory, and aim to identify the selective forces acting on this species in its putative 'enemy-free space' (Jeffries & Lawton, 1984). To quantify herbivory experienced by typical Brassicaceae species under these same field conditions, we use the annual *Rhamnospermum nigrum* (syn. *Brassica nigra*) as a phytometer (Clements & Goldsmith, 1924). Phytometers are standardized, transplanted plant species used as 'measuring instruments' to compare environments, and they are commonly used to assess herbivore pressure across sites and years (Scherber et al., 2006). *R. nigrum* is a representative Brassicaceae species that is well-liked by glucosinolate-resistant herbivores, and which shares a similar phenology, growth rate, and size with *E. cheiranthoides* under field conditions. Although the two species are phylogenetically distant, *R. nigrum* may thus functionally resemble a cardenolide-free ancestor of *E. cheiranthoides.*

Plants were grown in fields adjacent to oilseed rape (*Brassica napus*), which provided a high density of Brassicaceae-associated herbivores. We monitored herbivore abundance and plant damage across full growing seasons in two years. In the second year, we additionally applied insecticide treatments to manipulate herbivore pressure, and we included a competition treatment to assess how herbivory and defence interact to influence plant performance. We hypothesise that the novel cardenolide defence renders *E. cheiranthoides* better protected and less damaged by herbivores than *R. nigrum*, resulting in higher fitness. Conversely, we predict that under low herbivore pressure, the dual investment in defence may make *E. cheiranthoides* competitively inferior to *R. nigrum*.

2. Methods

2.1 Plant material

Erysimum cheiranthoides is an annual plant that is native to central and northern Europe and parts of Asia (Polatschek, 2010, 2013), where it grows in scattered populations in ruderal habitats. Plants commonly flower from May through September, with peak flowering in June and seed ripening in August to October (Polatschek, 2013; anonymous authors, personal observations). We grew a set of natural accessions of *E. cheiranthoides* (‘genotypes’ hereafter) from locations in western and central Europe in two common garden experiments in Switzerland in 2022 and 2023. A total of 38 genotypes were used in the first experiment, but due to large phenological variation among genotypes, we only used subset of nine late-flowering genotypes for the second experiment. All genotypes had been propagated in a common greenhouse environment for two generations before use. Seeds of *R. nigrum* used in this study were originally provided by the Botanical Garden of Krefeld, Germany.

Plants for field experiments were sown in late April for transplantation to the field in late May. We soaked seeds of *E. cheiranthoides* in water and kept them at 4 °C for three days to break dormancy. Three soaked seeds were placed on the soil surface of pots (7 × 7 × 8 cm) filled with a 1:1 mixture of sand and peat-based planting substrate (Einheitserde, Patzer Erden GmbH, Germany). Seeds of *R. nigrum* were directly sown into pots without pre-treatment and lightly covered with soil. Pots were covered with transparent plastic hoods for one week to maintain high humidity, and seeds were germinated in a growth chamber (constant light, 23 °C, 60% relative humidity). Seven days after sowing, plants were moved to an open greenhouse and shaded from direct sunlight for continued growth and hardening. In the last week of May, three-week old plants were transplanted into freshly tilled fields at the Swiss federal agricultural research station (Agroscope Reckenholz, Switzerland). Plants were transplanted to the field inside their plastic pot to slow the escape of growing roots and to limit excessive biomass growth in the field. A small set of plants was kept in the greenhouse for an additional week and used for the assessment of leaf traits (trichome density and trichome size) and innate herbivore preference under laboratory conditions (see Supplementary Methods).

2.2 Field experiments

2.2.1 Field experiment 2022

In 2022, we used a rectangular field site measuring 6 m × 80 m in a SW to NE orientation (Supplementary Figure S1a, 47.4376° N, 8.5268° E), located alongside a larger field of oilseed rape (*Brassica napus*). On either side of the experimental plot, 1 m-wide buffer strips of a commercial cover crop mixture consisting of *Raphanus sativus* and *Avena strigosa* had been sown two months earlier. We divided the experimental plot into ten blocks (5 × 7 m), and in each block we planted 38 *E. cheiranthoides* and four *R. nigrum* plants in a randomized grid pattern, with plants spaced 1 m apart and with a 0.5 m distance to the plot edge on each side. Throughout the experiment, plants were watered as needed, and the surrounding soil was weeded regularly and kept free of other vegetation. Unfortunately, buffer strips had to be mowed halfway through the experiment (week 5) to prevent weed seed dispersal.

We closely monitored plants over a period of nine weeks. In weeks 3, 6, and 9, we assessed plant damage by herbivores, and in the six remaining weeks, we recorded the herbivores that were present on each experimental plant. In weeks of herbivore community assessments, we visited each plant once and recorded the type and number of herbivores sitting or feeding on the plant. Herbivores were recorded at species level where visual identification was feasible, and as functional groups otherwise (e.g., flea beetles, weevils). Assessment of all plants was completed over 2-3 consecutive days in each week. In weeks of damage assessment, we visited each plant once to record leaf damage and plant size. We approximated total damage by counting the number of leaves on a plant with visible herbivore damage of any size, and we approximated plant size by counting the total number of leaves and measuring plant height. A representative sample of leaves were harvested and analysed to determine nutritional quality of plants throughout the 2022 experiment (see Supplementary Methods).

Whole plants were sequentially harvested for biomass, with complete blocks assigned to different harvests. Plants in blocks 1-3 were harvested in week 8 to capture early plant biomass, mostly before seed setting. Plants in blocks 4-6 were harvested in week 11, and plants in blocks 8-10 were harvested in week 14. For biomass harvesting, we cut the stem of each plant at soil level and placed the entire aboveground biomass in paper bags. Aboveground biomass was dried at 60 °C for

48-96 hours and weighed to the nearest mg. The entire block 7 was randomly selected for plants to complete development to seed production. To prevent seed loss in the exposed field site, plants were removed from the field in week 8 and transported back to a greenhouse. At the onset of seed ripening, plants were individually wrapped in paper bags to capture scattered seeds. Plants were harvested when seeds were fully ripe, at which point we separated seeds from vegetative biomass, dried the biomass at 60 °C, and weighed plant and seed mass separately. Finally, we counted and weighed a subset of 100 seeds for each plant to determine average seed size.

2.2.2 Field experiment 2023

Based on the results of the 2022 field experiment, we set up a modified field experiment in 2023 with added treatments of plant competition and herbivore suppression. To test for the effect of plant-plant competition, a subset of *E. cheiranthoides* plants was grown together with a *R. nigrum* plant in the same 7 x 7 x 8 cm pot. To reduce herbivore loads, half of all plants (individual and competing) were additionally treated with weekly applications of lambda-cyhalothrin (Kendo® Gold, Maag Gardens, Switzerland), a non-systemic pyrethroid insecticide.

In 2023, we used a different rectangular field site measuring 4 m × 66 m in a W to E orientation (Supplementary Figure S1b, 47.4284° N, 8.5232° E), again located alongside a larger field of oilseed rape (*Brassica napus*). On either side of the experimental plot, 1.5 m-wide buffer strips of the same cover crop mixture had been sown one week prior to transplanting, which were maintained throughout the experiment. We divided the experimental plot into six blocks (3 × 7 m). For blocks 1, 2, 5, and 6, we planted 36 individual *E. cheiranthoides* and 4 *R. nigrum* plants each in a stratified random grid pattern, with plants spaced 1 m apart and with a 0.5 m distance to the plot edge on each side. For blocks 3 and 4, we planted 40 paired *E. cheiranthoides* and *R. nigrum* plants each, with each pair spaced apart from the next by 1 m (Supplementary Figure S1b). Starting at transplanting, we applied weekly sprays of lambda-cyhalothrin (15 mg/L water) to all plants in blocks 2, 4, and 6, completely wetting all leaf surfaces. We maintained spraying for seven consecutive weeks, increasing the total volume sprayed as plants were growing larger, from approximately 30 mL per plant in the

first three weeks up to 150 mL per plant by week 7. Plants in blocks 1, 3, and 5 were sprayed with an equivalent amount of water.

Herbivore community assessments were carried out on individual plants as before (weeks 1, 2, 4, 5, 7, 8), while for competing plants we could only assess herbivore communities in the first half of the experiment. Damage was assessed on all plants (individual plants: weeks 3, 6, 9; competing plants: weeks 3, 6) using a modified approach to distinguish leaves with high (leaves with more than 75% of area damaged), low, and no damage. Plant height was measured weekly with both assessments, while during damage assessments, we also measured plant diameter and branch number. In 2022, total leaf counts had high levels of observer bias for older plants, thus for weeks 6 and 9 in the 2023 experiment, we only counted the total number of leaves on 20 randomly selected plants and used predictive models to estimate leaf number for the remaining plants (see Supplementary Methods). All plants were harvested in week 10 by cutting the stems at soil level and placing the entire aboveground biomass in paper bags, followed by drying at 60°C for 48-96 hours and weighing to the nearest mg.

2.3 Statistical analyses

The current study is focused on differences between *E. cheiranthoides* and *R. nigrum*, while the description of intraspecific variation among *E. cheiranthoides* genotypes is published elsewhere (anonymous authors, in preparation). However, we account for potential differences among plant genotypes here by including plant genotype as a random effect in all analyses. We use intraclass correlation coefficients (ICC, function *icc*, R package ‘performance’; Lüdecke et al., 2021) to quantify genotype contribution to variation in each trait. To ensure comparability between years, we only use data for *E. cheiranthoides* from the nine genotypes grown in both years of field experiments (and all data for *R. nigrum*). All analyses were performed in the statistical software R v.4.5.1 (R Core Team, 2023).

2.3.1 Herbivore community composition and phenology

To compare herbivore community composition between the two plant species, we first analysed total herbivore abundance summed across each year and compared community composition during peak abundance using multivariate analyses (see Supplementary Methods). To examine temporal variation in herbivore presence and abundance, we then used a series of generalised additive models (GAMs, function *gam*, R package 'mgcv'; Wood et al., 2016), which model nonlinear responses across time using thin-plate regression splines. Given the differences in experimental design between 2022 and 2023, we performed separate analyses for each year. Two sets of GAMs were fit for each of the eight major herbivore species or species groups. First, we fitted binomial GAMs to presence-absence data across all six weeks of observations, and second, we excluded weeks with zero observations for each herbivore and fitted negative binomial GAMs to abundance data of the remaining weeks.

For the 2022 experiment, we constructed pairs of nested GAMs that shared a fixed effect of plant species but differed by their temporal smoothers: one model assuming a shared temporal pattern across plant species, and the other allowing plant-specific smoothers. Both models included random intercepts for plant genotype and plant identity nested within genotype. For binomial GAMs, the number of smoother nodes (parameter k) was fixed to 5, whereas for negative binomial GAMs, k was set to $W_{pres} - 1$, where W_{pres} is the number of observation weeks with herbivore presence. Nested models differing in the smoothing structure were fitted using maximum likelihood (ML) and compared via Akaike's Information Criterion (AIC), preferring the simpler model unless ΔAIC was >2. The optimal model was then refitted using restricted maximum likelihood (REML), and significance of fixed effects was evaluated using Wald tests on explained deviance.

For the 2023 experiment, we followed a similar approach but also included plants of the insecticide treatment. To determine optimal model structure for each herbivore, we first compared nested models differing in their fixed effects, including either additive or interactive effect of plant species and insecticide, while allowing smoothers to vary across all four combinations of the two factors. We then fixed the optimal fixed-effects structure (based on AIC) and compared nested models differing in the temporal smoother (global, by plant species, by insecticide, or by their combination).

2.3.2 Plant damage assessments

Leaf damage was analysed using binomial generalized linear mixed-effects Models (GLMMs, function *glmer*, R package 'lme4'; Bates et al., 2015) fitted to the proportion of damaged leaves. For the 2022 field experiment, the numbers of damaged and undamaged leaves per plant were used as a two-vector response variable, representing the proportion of leaves with insect damage. This binary response was modelled using fixed effects of assessment week, plant species, and their interaction, an additive fixed effect of observer, and random intercepts for plant identity and plant genotype. We assessed significance of fixed effects using Type III Wald X^2 tests (function *Anova* in R package 'car'; Fox & Weisberg, 2019), and post hoc pairwise comparisons (Tukey's HSD; $\alpha = 0.05$) were performed using *emmeans* (R package emmeans; Lenth, 2023).

For the 2023 field experiment we used a similar approach, but because damage levels were overall higher in this experiment, we used a two-vector response of highly damaged leaves (defined as > 75% leaf area damaged) *vs.* undamaged and lightly damaged leaves to avoid issues with zero variance in *R. nigrum*. This response was modelled using fixed effects of assessment week, plant species, insecticide treatment, and competition treatment, including all possible interactions. Because damage was not assessed in the competition treatment in week 9, we could not include a four-way interaction, thus for the competition treatment, we only specified interactions with plant species and insecticide treatment. We again specified observer as an additive fixed effect, and included random intercepts for plant identity, neighbourhood group (grouping together paired plants of the competition treatment), and plant genotype. Post-hoc pairwise comparisons for both models were performed using *emmeans.*

2.3.3 Effects of herbivory and competition on plant growth

Herbivore numbers dropped substantially following the early mowing of buffer strips in the 2022 field experiment. To test whether this reduction in herbivore pressure influenced plant growth, we quantified growth using repeated plant height measurements taken in weeks 3, 6, and 9. We also used a similar analysis of weekly height measurements in 2023 to assess the effect of insecticide application on growth (see Supplementary Methods).

For the 2022 field experiment, we analysed the biomass of plants harvested in weeks 8, 11, and 14 using a linear mixed effects model (*lmer*, R package 'lme4'; Bates et al., 2015). Ln-transformed dry biomass was modelled using fixed effects of plant species, harvest week, and their interaction, and a random intercept of plant genotype. For the 2023 field experiment, we modelled ln-transformed plant biomass of plants (all harvested after 10 weeks) using fixed effects of plant species, insecticide treatment, competition treatment, and their interactions as fixed effects, with random intercepts for plant genotype and neighbourhood group. Post-hoc pairwise comparisons for both models were again performed using *emmeans*.

3. Results

3.1 Herbivore community composition and phenology

Across two consecutive years of field experiments, we recorded 11 herbivore species or species groups, reflecting a consistent herbivore community within the oilseed rape-dominated landscape. All herbivores were found on both plants in both years, except for a few low-abundance species missing from either *R. nigrum* or *E. cheiranthoides* in 2023. Nevertheless, most herbivores were markedly more abundant on *R. nigrum* than on *E. cheiranthoides* (Supplementary Tables S1-S2). Unexpectedly, the insecticide treatment applied in 2023 did not uniformly reduce herbivore abundance. While flea beetles and crucifer shield bugs (*Eurydema* spp.) were less common on insecticide-treated *E. cheiranthoides*, pollen beetles, cabbage whiteflies, and weevils were more common on treated *R. nigrum*, and aphids were more abundant on treated plants of both species (Supplementary Table S2).

Despite the shared herbivore community, community composition (estimated using Bray-Curtis dissimilarities) differed substantially across plant species, treatments, and years (see Supplementary Results, Figure S2). Generalized additive models (GAMs) of herbivore presence and abundance further revealed pronounced seasonal dynamics, yet broadly similar temporal patterns emerged across the two study years. In both years, aphids and flea beetles were the first herbivores to colonize experimental plants, arriving earlier and reaching higher numbers on *R. nigrum* than on *E. cheiranthoides* (Figure 1, Supplementary Figure S3). By week 4, pollen beetles occurred in high

numbers on non-flowering *R. nigrum* and, to a lesser extent, on *E. cheiranthoides* (Figure 1), whereas most other herbivores reached their peak abundance by week 5. Six of the eight main herbivores were more abundant on *R. nigrum* in 2022, and this pattern remained consistent for four of these species in 2023 (Figure 1, Supplementary Table S4). The only exceptions were crucifer shield bugs and cabbage whiteflies, which occurred at similar frequencies on both plant species. Across all GAMs, the proportion of variance attributable to plant genotype effects was relatively modest (ICC = 0 – 25.8 % across models; Supplementary Table S4).

In 2022, most herbivores declined sharply in abundance during the second half of the experiment (Figure 1). This decline likely resulted from the early mowing of buffer strips adjacent to the experimental plot, as no comparable decline was observed in 2023, when buffer strips remained intact until the end of the experiment. Analyses of insecticide-treated plants in 2023 further elucidated the unexpected increase of some herbivores under sprayed conditions (Supplementary Figure S4). Herbivores that increased under insecticide treatment not only reached higher peak abundances but also persisted for longer on these plants, as indicated by models with treatment-specific smoothers being better supported by AIC (Supplementary Table S4).

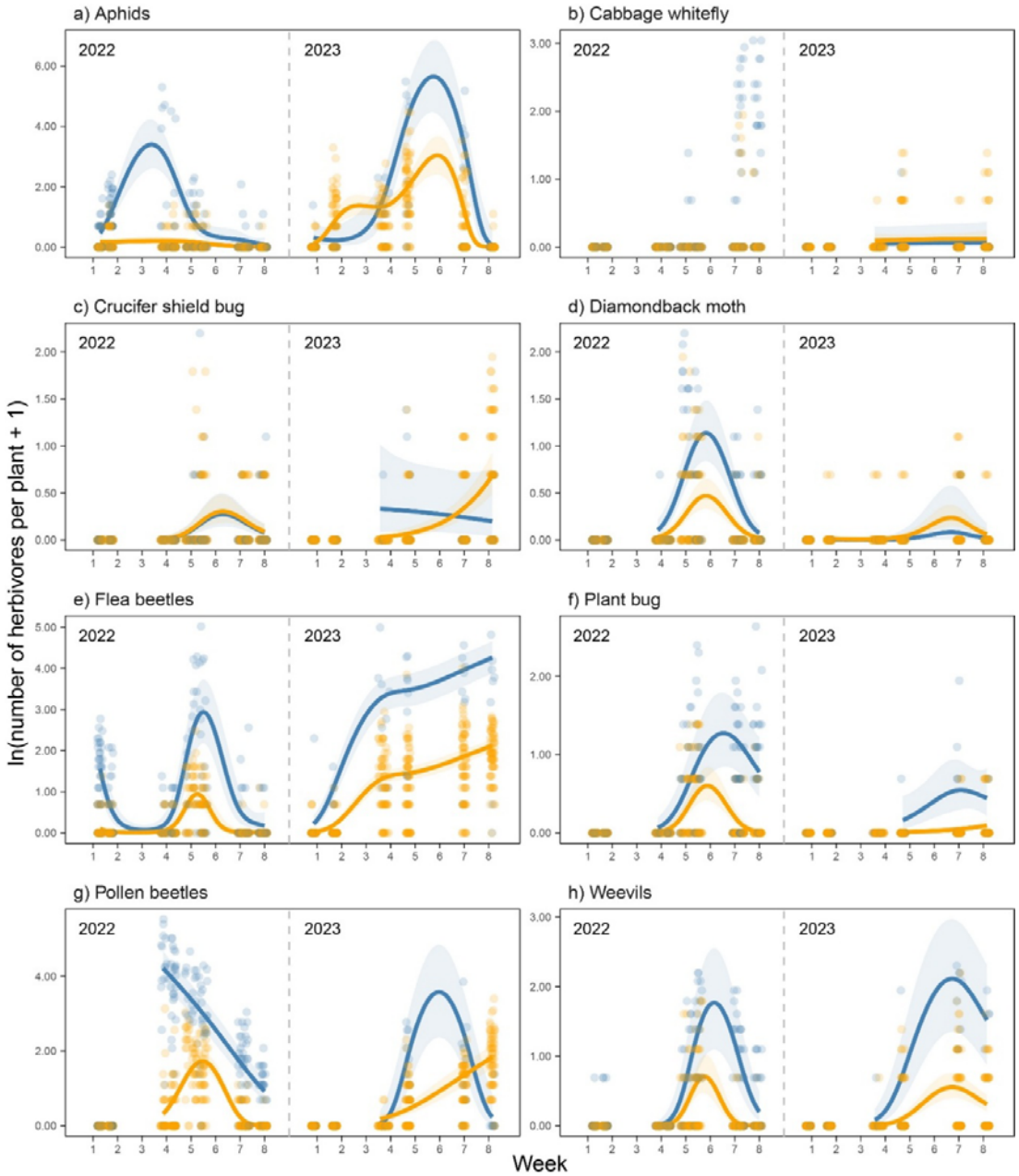

Figure 1. Herbivore abundance for the eight main herbivores observed on *R. nigrum* (blue) and *E. cheiranthoides* (orange) in the 2022 and 2023 field experiments. Points represent observations on individual plants, while lines and shaded areas show mean model predictions and 95% confidence intervals from negative binomial generalized additive models (GAMs). GAMs were fitted to count data after exclusion of weeks with zero observations. Each panel (a-h) shows result for a single herbivore, with separate models fitted for each year. All models used 'days in the field' as temporal variable, but the x-axes show 'week' for easier comparison with other results. No model could be fit for cabbage whiteflies in 2022 due to insufficient observations on *E. cheiranthoides*. See Supplementary Table S4 for test statistics of each model.

3.2 Plant damage

Leaf damage on *R. nigrum* was substantially higher than on *E. cheiranthoides* in the 2022 field experiment (Figure 2) and varied significantly by plant species and week (Supplementary Table S5a), with a modest proportion of variance attributable to plant genotype effects (ICC = 6.7 %). Damage to *R. nigrum* was almost complete in weeks 3 and 6 (i.e., all leaves had some damage). In contrast, less than 30% of leaves were damaged on *E. cheiranthoides*, and damage further decreased by week 6 (week 3 vs. 6: z-ratio = 12.30, $p < 0.001$). Damage decreased on both species by week 9 (week 6 vs. 9, *R. nigrum*: z-ratio = 10.33, $p < 0.001$; *E. cheiranthoides*: z-ratio = 18.76, $p < 0.001$), mirroring the decline observed in herbivore abundances towards the end of the experiment.

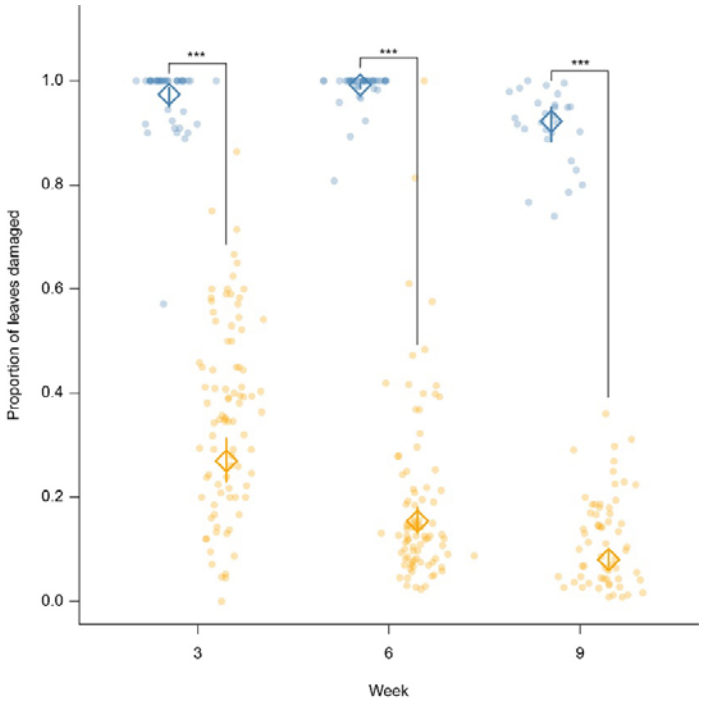

Figure 2. The proportion of damaged plants in plants of the 2022 field experiment. Points are values for individual plants, while diamonds and vertical lines are the means and 95% confidence intervals from a binomial GLMM. Brackets highlight significant linear contrasts within each week at the $p < 0.05$ level.

In the 2023 field experiment, quantified leaf damage on *R. nigrum* plants exposed to ambient herbivory was again almost complete. The proportion of heavily damaged leaves (leaves with more than 75% area damaged) was substantially higher on *R. nigrum* compared to *E. cheiranthoides* across all weeks (Figure 3), but relative amounts varied significantly across time and treatments (Supplementary Table S5b, plant genotype ICC = 4.3 %). Under ambient herbivory, damage levels remained relatively constant, only slightly decreasing in week 6 (week 3 vs. 6, *R. nigrum*: z-ratio = 6.82, $p < 0.001$; *E. cheiranthoides*: z-ratio = 22.64, $p < 0.001$), before increasing again in week 9 (week 6 vs. 9, *R. nigrum*: z-ratio = -2.41, $p = 0.042$; *E. cheiranthoides*: z-ratio = -27.94, $p < 0.001$). Insecticide treatment strongly reduced damage on *E. cheiranthoides* plants in weeks 3 and 6, while this effect disappeared by week 9 (Figure 3). In contrast, insecticide only significantly reduced damage on *R. nigrum* in week 9 (Figure 3). Interestingly, while plant-plant competition did not significantly affect damage under ambient herbivory, the competition treatment amplified the effect of the insecticide treatment and reduced damage levels below those of the insecticide treatment alone in weeks 3 for *E. cheiranthoides*, and in week 6 for both plant species (Figure 3). Week 9 lacked damage quantifications on competing plants; thus, competition contrasts could not be estimated for the final observation.

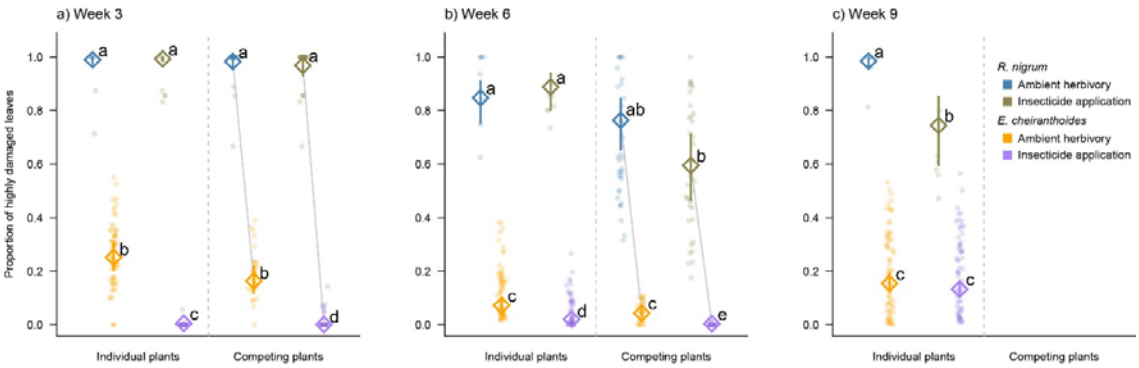

Figure 3. The proportion of highly damaged leaves (leaves with more than 75% area damaged) on plants in a) week 3, b) week 6, and c) week 9 of the 2023 field experiment. Points are values for individual plants, while diamonds and vertical lines are the means and 95% confidence intervals from a binomial GLMM. Letters highlight significant linear contrasts at the $p < 0.05$ level within each week. Means of plants in the competition

treatment are connected by grey lines to show the paired experimental design. In week 9, damage was only quantified on individual plants.

3.3 Plant growth and competition

To better understand herbivore impact on plant growth, we modelled plant height over time using sequential height measurements. In 2022, we found clear differences in height growth between *R. nigrum* and *E. cheiranthoides* (Supplementary Figure S5a, Supplementary Table S6a). During the period of peak herbivore abundance (weeks 3-6), *R. nigrum* only minimally increased in height (absolute growth rate: 0.32 [0.30 – 0.34] cm day^{-1}; mean [95% confidence interval]), while *E. cheiranthoides* grew more than five times faster (1.71 [1.62 – 1.79] cm day^{-1}). Growth of *R. nigrum* increased towards the end of the experiment, and between weeks 6 and 9, both species exhibited similar growth rate (*R. nigrum*: 1.34 [1.24-1.42] cm day^{-1}; *E. cheiranthoides*: 1.58 [1.50 – 1.65] cm day^{-1}).

To test whether the late increase in *R. nigrum* growth was causally linked to declining herbivore pressure, we compared growth rates between insecticide-treated and control plants in 2023 (Supplementary Figure S5b-c). Both species grew faster under the insecticide treatment (Supplementary Table S6b), with sprayed *R. nigrum* growing more than twice as fast between weeks 6 and 9 compared to unsprayed controls (ambient herbivory: 0.47 [0.15 – 0.98] cm day^{-1}; sprayed: 1.03 [0.36 – 1.93] cm day^{-1}). Note that the large uncertainty and overlapping confidence intervals likely reflects the small sample size for *R. nigrum* in the 2023 experiment (n = 7 per treatment).

The observed patterns in height growth directly translated into differences in aboveground biomass. In the 2022 field experiment, differences in biomass between species shifted between early and later harvests (Supplementary Table S7a), with a considerable proportion of variance attributable to plant genotype effects (ICC = 24.8 %). At the first harvest (week 8), *R. nigrum* had significantly lower biomass than *E. cheiranthoides* (Figure 4a, t-ratio = -3.02, p = 0.017). However, mirroring the increased growth rate of *R. nigrum* in the second half of the experiment, this difference had disappeared by weeks 11 and 14.

In the 2023 field experiment, all plants were harvested in week 10, and we detected a significant three-way interaction among plant species, insecticide treatment, and competition (Figure 4b, Supplementary Table S7b, plant genotype ICC = 8.4 %). For individually grown plants under ambient herbivory, biomass of *R. nigrum* was close to zero, whereas *E. cheiranthoides* appeared largely unaffected. Although insecticide application did not consistently remove herbivores and only partially reduced visible damage on *R. nigrum* (Figure 3), sprayed *R. nigrum* plants reached substantially higher biomass. In contrast, *E. cheiranthoides* showed no comparable benefit from insecticide treatment. Interestingly, the effects of interspecific competition depended on insecticide treatment. Under ambient herbivory, biomass of *R. nigrum* was further reduced when grown in competition, while biomass of *E. cheiranthoides* remained unchanged. Under insecticide treatment, *R. nigrum* reached similar biomass regardless of competition, whereas *E. cheiranthoides* showed a marked reduction in biomass when grown in competition – likely due to growth suppression from the less-attacked *R. nigrum* plants. Although we did not directly measure plant fitness in 2023, we found a strong positive correlation between aboveground biomass and seed production for *E. cheiranthoides* in 2022 (Supplementary Figure S6), suggesting that growth suppression by competition would likewise reduce fitness.

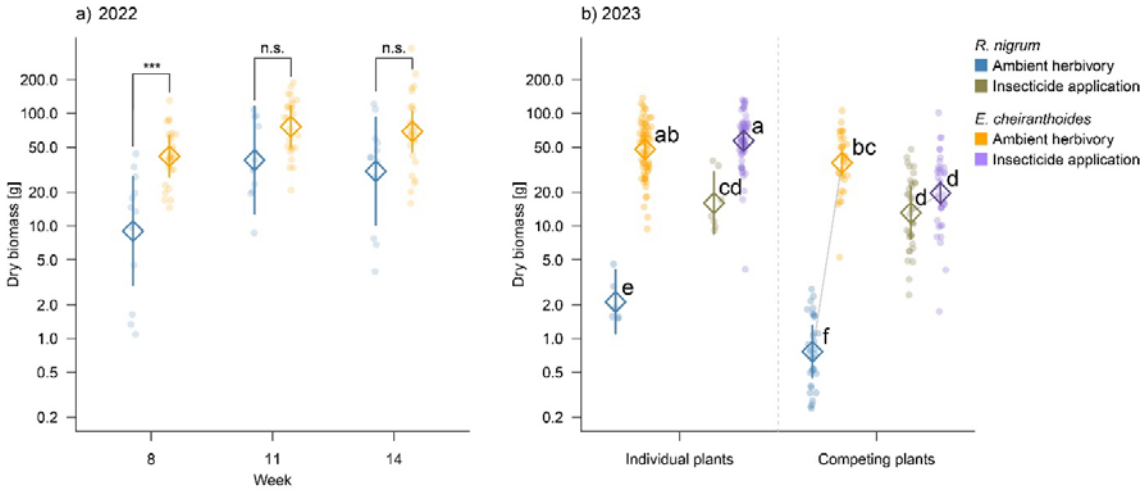

Figure 4. a) Total aboveground biomass of subsets of plants harvested after 8, 11, and 14 weeks in the 2022 field experiment. Diamonds and lines are means and 95% confidence intervals from a linear model. Brackets highlight significant linear contrasts within each week at the $p < 0.05$ level. b) Biomass of individual (left) and

competing (right) *R. nigrum* and *E. cheiranthoides* plants harvested after 10 weeks of growth in the 2023 field experiment. Plants were growing individually or as conspecific pairs in buried pots, separated from the nearest neighbour by 0.5 m in all directions. Points are individual plant values, while diamond symbols and lines are means and 95% confidence intervals from a linear mixed-effects model. Letters denote significant linear contrasts at the $p<0.05$ level.

3.4 Plant traits and innate herbivore preference

The two plant species used in this experiment naturally differ in a wide range of other traits besides cardenolide production. Nutritional traits quantified in the 2022 field experiment showed consistent but modest differences between the two species (see Supplementary Results, Figure S7). In contrast, trichome density and size varied substantially, with leaves of *E. cheiranthoides* being densely covered in small trichomes on both sides, while *R. nigrum* primarily expressed larger trichomes along leaf veins on the underside of its leaves (see Supplementary Results, Figure S8). We further compared the role of leaf trait differences on innate herbivore preference using cut leaf disc choice assays under controlled laboratory conditions. Of the four tested Brassicaceae herbivores (two of which we also observed feeding in the field), each significantly preferred *R. nigrum* over *E. cheiranthoides* (Supplementary Figure S9). Interestingly, this preference was least pronounced for *E. ornata*, mirroring the weaker preference for *R. nigrum* of this herbivore in the field.

4. Discussion

The dually defended *E. cheiranthoides* was attacked by substantially fewer herbivores than its Brassicaceae relative *R. nigrum* across two field seasons. Herbivores caused severe leaf damage to *R. nigrum*, and growth of *R. nigrum* was almost completely suppressed when insect herbivores were abundant. In contrast, even during peak abundance, the limited damage on *E. cheiranthoides* had no detectable impact on plant growth, consistent with an escape from herbivore-imposed selection. Manipulating herbivore abundance and plant-plant competition further revealed not only an absence of negative herbivore effects on *E. cheiranthoides*, but even a net benefit of herbivore pressure under intense competition. When growth suppression of *R. nigrum* by herbivores was experimentally

reduced, increased competition from *R. nigrum* halved *E. cheiranthoides* growth, indicating that the defensive superiority of *E. cheiranthoides* is paired with comparatively weak competitive ability.

Although our analyses compare only two plant species that only rarely co-occur in nature, the role of *R. nigrum* in our study should be interpreted as a phytometer – a standardized, glucosinolate-defended Brassicaceae species used to gauge background herbivore pressures and the competitive context typical for Brassicaceae communities. We chose *R. nigrum* because it is broadly attractive to glucosinolate-tolerant specialists and shares a similar phenology and size with *E. cheiranthoides* under our field conditions. *R. nigrum* thus primarily functions as a practical benchmark for 'cardenolide-free' Brassicaceae performance, intended to calibrate the magnitude of herbivory and competition that *E. cheiranthoides* experiences in nature. This framing also justifies some generalization from the relatively artificial pairwise comparison to broader inferences about enemy escape and defence costs.

Herbivores observed on both plant species were mostly Brassicaceae specialists tolerant of glucosinolates, likely originating from large source populations in the surrounding Brassicaceae crops and buffer strips, and 'spilling over' onto our plots (associational susceptibility; Barbosa et al., 2009). This landscape effect is illustrated by the sharp decline in herbivores following the premature mowing of buffer strips in 2022 (oilseed rape crops having been harvested even earlier). However, even though we intentionally selected a Brassicaceae-dominated environment to ensure high specialist herbivore pressures, specialist dominance on Brassicaceae plants is common in field studies (Bidart-Bouzat & Kliebenstein, 2008; Mertens et al., 2021), likely because glucosinolates filter out many generalist herbivores (but see Zalucki et al., 2021).

Interestingly, we never recorded larvae of the cabbage white butterfly (*Pieris rapae*) on experimental plants despite the prevalence of adult butterflies (anonymous authors, personal observations). This absence on *E. cheiranthoides* is consistent with strong aversion of this species to cardenolides (Sachdev-Gupta et al., 1993) but surprising for *R. nigrum*. One possibility is field-scale associational resistance for *R. nigrum* arising from proximity to *E. cheiranthoides* (Atsatt & O'Dowd, 1976; Barbosa et al., 2009). Additional evidence for this comes from the competition experiment, where insecticide-treated *R. nigrum* paired with *E. cheiranthoides* received the least amount of

damage. Given that competition can elevate defence in some plants (Lankau & Kliebenstein, 2009), *R. nigrum* may have simultaneously benefitted from neighbour-mediated enemy reduction while suppressing *E. cheiranthoides* growth.

Most herbivores preferred *R. nigrum* over *E. cheiranthoides* regardless of feeding guild (e.g., caterpillars, flea beetles, aphids). An exception to this pattern were the crucifer shield bugs (*Eurydema spp.*), which occurred on both plant species at similar abundances. Although *Eurydema* commonly feed on different *Erysimum* species (Gómez, 2005) and *E. cheiranthoides* plants (anonymous authors, personal observations), laboratory choice assays still showed a slight preference for *R. nigrum*, and *Eurydema* remain broadly generalised across the Brassicaeae (Piersanti et al., 2020). It thus remains unresolved whether some *Eurydema* bugs actively prefer *Erysimum* under natural conditions, and whether this may represent early stages of specialization.

None of the observed herbivores exhibited complete avoidance of *E. cheiranthoides*, but importantly, we did not distinguish between perching and feeding in our counts. Highly mobile taxa (e.g., pollen beetles, flea beetles) may frequently alight on *E. cheiranthoides* but depart after brief sampling. High mobility may also explain higher counts for some herbivore species on insecticide-treated plants in 2023. Pyrethroid insecticides have low environmental persistence (Ripley et al., 2001), and weekly applications likely reduced damaging residents while also creating higher-quality leaves that attracted more transient, less damaging visitors. Consistent with such an effect, we found sprayed plants to be less damaged at least in some weeks, and to reach substantially higher biomass than untreated controls.

Our two-species comparison of *R. nigrum* and *E. cheiranthoides* cannot by itself address the causal role of cardenolides in plant defence, as naturally, many more traits vary between the two species. Nonetheless, we evaluated a set of additional traits that may contribute to herbivore preference. We observed only modest differences in leaf nutrient content for most of season, whereas trichome type and density differed more strongly. Trichomes often play a role in plant defence against insects (Levin, 1973; Sato et al., 2019), and may be particularly important for the *Erysimum* system (Wang et al., 2025). Additional structural or morphological traits might perhaps affect plant apparency and herbivore host perception (Strauss et al., 2015), but these are less likely to explain the

consistent preference of different herbivores for *R. nigrum* leaf choice assays. Overall, the magnitude and consistency of herbivore preference are unlikely to be caused by modest nutritional differences or plant shape alone. Cardenolides remain a key distinguishing trait between the two species, though additional roles for trichomes and other unmeasured traits cannot be excluded.

A direct causal role for cardenolides in *E. cheiranthoides* defence was recently demonstrated using CRISPR/Cas9 knockouts lacking cardenolides (Younkin et al., 2024). Several specialist herbivores, including *P. rapae*, increased feeding on knockouts while avoiding wildtype plants. Other herbivores, such as flea beetles and aphids, showed weaker or inconsistent responses, while *P. xylostella* appears to lack a cardenolide response entirely (Wang & Züst, 2025). These findings suggest that cardenolides function as potent qualitative defences against some herbivores and weaker quantitative – or even ineffective – defences against others.

Across all our analyses, the proportion of variance attributable to *E. cheiranthoides* genotype (intra-population variation) was moderate, with intraclass correlation coefficients (ICC) typically around 5%, but reaching up to 25% for individual responses (e.g., pollen beetle abundance). This degree of variation indicates substantial standing genetic diversity in growth- and defence-related traits among *E. cheiranthoides* genotypes. Such variation may provide the raw material for natural selection to fine-tune defence allocation or cardenolide composition and could help buffer populations against fluctuating herbivore pressures. Future work parsing the intraspecific variation in cardenolide concentrations and composition could clarify how genotype-level diversity contributes to differences in field damage.

While *E. cheiranthoides* largely escaped a negative impact of herbivory, concurrent production of glucosinolate and cardenolide defences likely incurs substantial allocation cost. Trade-offs between resistance and growth are common (Züst & Agrawal, 2017) but can be masked (Koricheva et al., 2004). Both the production of glucosinolates (in *Arabidopsis thaliana*) and cardenolides (in *Asclepias syriaca*) can reduce growth under some conditions (Züst et al., 2011, 2015). Producing both suites of defences therefore likely imposes large costs that should be apparent under most environmental conditions, which could explain the weak competitive ability of *E. cheiranthoides* we observed. However, under high herbivory, this strategy appears to pay off: while

damage by herbivores can reduce growth of undefended plants directly by reducing leaf area and depleting resources (Machado et al., 2016) or induce defences at a cost of reduced growth (Attaran et al., 2014; Zangerl et al., 2002), *E. cheiranthoides* remained unimpaired. Preferential herbivore attack on the competitively superior but susceptible Brassicaceae community (represented by phytometer *R. nigrum*) therefore indirectly promotes the resistant species, and would be expected to result in an increase in its frequency over time if herbivore pressure was constant (Crawley, 1989; Myers & Sarfraz, 2017).

Despite weak competitive ability in the absence of specialized herbivores, the genus *Erysimum* has undergone a recent radiation that coincided with the gain of cardenolides (Züst et al., 2020), suggesting that an escape from herbivory aided diversification in enemy-free space. Even so, *Erysimum* species typically occupy spares, marginal habitats and rarely dominate communities. Further evolutionary tuning may reduce defence for these plants in the future (e.g., Karasov et al., 2017), but increased *Erysimum* abundance could also intensify selection for cardenolide resistance in herbivores (Dobler et al., 2012; Petschenka et al., 2017), thus perpetuating the arms race between plants and their herbivores.

In conclusion, the gain of a novel defence appears to have allowed *Erysimum* plants to escape herbivore-imposed selection – if not herbivory entirely. However, maintaining this 'enemy-free space' is costly, such that *Erysimum* thrives primarily where competitors are scarce or suppressed by herbivores. As these specific conditions are rare, *Erysimum* is currently confined to survive in marginal habitats, yet changing environmental conditions might well favour this unusually well-defended plant in the future.

Acknowledgements

We thank Mark Charran, Broti Biswas, Teresa Vaello, Daniel Schlagenhauf, Alina Pfammatter and Paul Wieduwilt for field assistance, and Laura Dällenbach, Rayko Jonas and Markus Meierhofer for greenhouse support. We are grateful to Agroscope Reckenholz for the use of their field sites and infrastructure, and we especially thank Daniel Fuchs and Friedrich Käser for invaluable assistance in the field, and Robert Baur for administrative support. Two anonymous reviewers provided valuable

feedback on an earlier version of this manuscript. This project has received funding from the European Research Council (ERC) under the European Union's Horizon 2020 research and innovation programme (grant agreement No 950319). Additional support was provided by a Swiss National Science Foundation grant PCEFP3_194590 to TZ and a grant of the Georges and Antoine Claraz Foundation.

References

Agrawal, A. A., Hastings, A. P., Johnson, M. T. J., Maron, J. L., & Salminen, J.-P. (2012). Insect herbivores drive real-time ecological and evolutionary change in plant populations. *Science*, *338*, 113–116.

Agrawal, A. A., Petschenka, G., Bingham, R. A., Weber, M. G., & Rasmann, S. (2012). Toxic cardenolides: Chemical ecology and coevolution of specialized plant–herbivore interactions. *New Phytologist*, *194*(1), 28–45. https://doi.org/10.1111/j.1469-8137.2011.04049.x

Atsatt, P. R., & O'Dowd, D. J. (1976). Plant defense guilds. *Science (New York, N.Y.)*, *193*(4247), 24–29. https://doi.org/10.1126/science.193.4247.24

Attaran, E., Major, I. T., Cruz, J. A. J., Rosa, B. A., Koo, A. J. K., Chen, J., Kramer, D. M., He, S. Y., & Howe, G. A. (2014). Temporal dynamics of growth and photosynthesis suppression in response to jasmonate signaling. *Plant Physiology*, *165*(3), 1302–1314. https://doi.org/10.1104/pp.114.239004

Barbosa, P., Hines, J., Kaplan, I., Martinson, H., Szczepaniec, A., & Szendrei, Z. (2009). Associational resistance and associational susceptibility: Having right or wrong neighbors. *Annual Review of Ecology, Evolution, and Systematics*, *40*(1), 1–20. https://doi.org/10.1146/annurev.ecolsys.110308.120242

Bates, D., Mächler, M., Bolker, B., & Walker, S. (2015). Fitting linear mixed-effects models using lme4. *Journal of Statistical Software*, *67*(1). https://doi.org/10.18637/jss.v067.i01

Bekaert, M., Edger, P. P., Hudson, C. M., Pires, J. C., & Conant, G. C. (2012). Metabolic and evolutionary costs of herbivory defense: Systems biology of glucosinolate synthesis. *New Phytologist*, *196*(2), 596–605. https://doi.org/10.1111/j.1469-8137.2012.04302.x

Bidart-Bouzat, M. G., & Kliebenstein, D. J. (2008). Differential levels of insect herbivory in the field associated with genotypic variation in glucosinolates in *Arabidopsis thaliana*. *Journal of Chemical Ecology*, *34*(8), 1026–1037. https://doi.org/10.1007/s10886-008-9498-z

Clements, F. E., & Goldsmith, G. W. (1924). *The phytometer method in ecology: The plant and community as instruments*. The Carnegie Institution of Washington.

Crawley, M. J. (1989). Insect herbivores and plant population dynamics. *Annual Review of Entomology*, *34*, 531–564. https://doi.org/10.1146/annurev.en.34.010189.002531

Dobler, S., Dalla, S., Wagschal, V., & Agrawal, A. A. (2012). Community-wide convergent evolution in insect adaptation to toxic cardenolides by substitutions in the Na,K-ATPase. *Proceedings of the National Academy of Sciences*, *109*(32), 13040–13045. https://doi.org/10.1073/pnas.1202111109

Edger, P. P., Heidel-Fischer, H. M., Bekaert, M., Rota, J., Glöckner, G., Platts, A. E., Heckel, D. G., Der, J. P., Wafula, E. K., Tang, M., Hofberger, J. A., Smithson, A., Hall, J. C., Blanchette, M., Bureau, T. E., Wright, S. I., dePamphilis, C. W., Eric Schranz, M., Barker, M. S., … Wheat, C. W. (2015). The butterfly plant arms-race escalated by gene and genome duplications. *Proceedings of the National Academy of Sciences*, *112*(27), 8362–8366. https://doi.org/10.1073/pnas.1503926112

Ehrlich, P. R., & Raven, P. H. (1964). Butterflies and plants: A study in coevolution. *Evolution*, *18*(4), 586–608. https://doi.org/10.1111/j.1558-5646.1964.tb01674.x

Fahey, J. W., Zalcmann, A. T., & Talalay, P. (2001). The chemical diversity and distribution of glucosinolates and isothiocyanates among plants. *Phytochemistry*, *56*, 5–51.

Fox, J., & Weisberg, S. (2019). *An R companion to applied regression* (Third Edition). Sage.

Gómez, J. M. (2005). Non-additive effects of herbivores and pollinators on *Erysimum mediohispanicum* (Cruciferae) fitness. *Oecologia*, *143*(3), 412–418. https://doi.org/10.1007/s00442-004-1809-7

Hambäck, P. A., & Beckerman, A. P. (2003). Herbivory and plant resource competition: A review of two interacting interactions. *Oikos*, *101*(1), 26–37. https://doi.org/10.1034/j.1600-0706.2003.12568.x

Herms, D. a., & Mattson, W. J. (1992). The dilemma of plants: To grow or defend. *The Quarterly Review of Biology*, *67*(3), 283. https://doi.org/10.1086/417659

Huang, X., Renwick, J. A. A., & Sachdev-Gupta, K. (1993). A chemical basis for differential acceptance of *Erysimum cheiranthoides* by two *Pieris* species. *Journal of Chemical Ecology*, *19*(2), 195–210. https://doi.org/10.1007/BF00993689

Jeffries, M. J., & Lawton, J. H. (1984). Enemy free space and the structure of ecological communities. *Biological Journal of the Linnean Society*, *23*(4), 269–286. https://doi.org/10.1111/j.1095-8312.1984.tb00145.x

Johnson, M. T. J. (2011). Evolutionary ecology of plant defences against herbivores: Plant defences against herbivores. *Functional Ecology*, *25*(2), 305–311. https://doi.org/10.1111/j.1365-2435.2011.01838.x

Karasov, T. L., Chae, E., Herman, J. J., & Bergelson, J. (2017). Mechanisms to mitigate the trade-off between growth and defense. *The Plant Cell*, *29*(4), 666–680. https://doi.org/10.1105/tpc.16.00931

Koricheva, J., Nykänen, H., & Gianoli, E. (2004). Meta-analysis of trade-offs among plant antiherbivore defenses: Are plants jacks-of-all-trades, masters of all? *The American Naturalist*, *163*(4), E64-75. https://doi.org/10.1086/382601

Lankau, R. A., & Kliebenstein, D. J. (2009). Competition, herbivory and genetics interact to determine the accumulation and fitness consequences of a defence metabolite. *Journal of Ecology*, *97*(1), 78–88. https://doi.org/10.1111/j.1365-2745.2008.01448.x

Lenth, R. V. (2023). *emmeans: Estimated Marginal Means, aka Least-Squares Means* (Version 1.8.8) [R (≥ 4.1.0)]. https://CRAN.R-project.org/package=emmeans

Levin, D. A. (1973). The role of trichomes in plant defense. *The Quarterly Review of Biology*, *48*(1, Part 1), 3–15. https://doi.org/10.1086/407484

Lüdecke, D., Ben-Shachar, M., Patil, I., Waggoner, P., & Makowski, D. (2021). performance: An R Package for Assessment, Comparison and Testing of Statistical Models. *Journal of Open Source Software*, *6*(60), 3139. https://doi.org/10.21105/joss.03139

Machado, R. A., McClure, M., Hervé, M. R., Baldwin, I. T., & Erb, M. (2016). Benefits of jasmonate-dependent defenses against vertebrate herbivores in nature. *eLife*, *5*, 1–21. https://doi.org/10.7554/eLife.13720

Mauricio, R., & Rausher, M. D. (1997). Experimental manipulation of putative selective agents provides evidence for the role of natural enemies in the evolution of plant defense. *Evolution*, *51*(5), 1435–1444. https://doi.org/10.2307/2411196

Mertens, D., Bouwmeester, K., & Poelman, E. H. (2021). Intraspecific variation in plant associated herbivore communities is phylogenetically structured in Brassicaceae. *Ecology Letters*, *24*, 2314–2327. https://doi.org/10.1111/ele.13852

Myers, J. H., & Sarfraz, R. M. (2017). Impacts of insect herbivores on plant populations. *Annual Review of Entomology*, *62*(1), 207–230. https://doi.org/10.1146/annurev-ento-010715-023826

Petschenka, G., Halitschke, R., Züst, T., Roth, A., Stiehler, S., Tenbusch, L., Hartwig, C., Moreno Gámez, J. F., Trusch, R., Deckert, J., Chalušová, K., Vilcinskas, A., & Exnerová, A. (2022). Sequestration of defenses against predators drives specialized host plant associations in preadapted milkweed bugs (Heteroptera: Lygaeinae). *The American Naturalist*, *199*(6), E211–E228. https://doi.org/10.1086/719196

Petschenka, G., Wagschal, V., Von Tschirnhaus, M., Donath, A., & Dobler, S. (2017). Convergently evolved toxic secondary metabolites in plants drive the parallel molecular evolution of insect resistance. *The American Naturalist*, *190*(S1), S29–S43. https://doi.org/10.1086/691711

Piersanti, S., Rebora, M., Ederli, L., Pasqualini, S., & Salerno, G. (2020). Role of chemical cues in cabbage stink bug host plant selection. *Journal of Insect Physiology*, *120*, 103994. https://doi.org/10.1016/j.jinsphys.2019.103994

Polatschek, A. (2010). Revision der Gattung *Erysimum* (Cruciferae): Teil 1. Russland, die Nachfolgestaaten der USSR (excl. Georgien, Armenien, Azerbaidzan), China, Indien, Pakistan, Japan und Korea. *Annalen Des Naturhistorischen Museums Wien B*, *111*, 181–275.

Polatschek, A. (2013). Revision der Gattung *Erysimum* (Cruciferae): Teil 5. Nord-, West-, Zentraleuropa, Rumänien und westliche Balkan-Halbinsel bis Albanien. *Annalen Des Naturhistorischen Museums Wien B*, *115*, 75–218.

R Core Team. (2023). *R Statistical Software*. (Version v4.3.1.) [Computer software].

Ratzka, A., Vogel, H., Kliebenstein, D. J., Mitchell-Olds, T., & Kroymann, J. (2002). Disarming the mustard oil bomb. *Proceedings of the National Academy of Sciences*, *99*(17), 11223–11228. https://doi.org/10.1073/pnas.172112899

Ripley, B. D., Ritcey, G. M., Harris, C. R., Denommé, M. A., & Brown, P. D. (2001). Pyrethroid insecticide residues on vegetable crops. *Pest Management Science*, *57*(8), 683–687. https://doi.org/10.1002/ps.325

Sachdev-Gupta, K., Radke, C. D., Renwick, J. A. A., & Dimock, M. B. (1993). Cardenolides from *Erysimum cheiranthoides*: Feeding deterrents to *Pieris rapae* larvae. *Journal of Chemical Ecology*, *19*(7), 1355–1369. https://doi.org/10.1007/BF00984881

Sato, Y., Shimizu-Inatsugi, R., Yamazaki, M., Shimizu, K. K., & Nagano, A. J. (2019). Plant trichomes and a single gene GLABRA1 contribute to insect community composition on field-grown Arabidopsis thaliana. *BMC Plant Biology*, *19*(1), 1–12. https://doi.org/10.1186/s12870-019-1705-2

Scherber, C., Mwangi, P. N., Temperton, V. M., Roscher, C., Schumacher, J., Schmid, B., & Weisser, W. W. (2006). Effects of plant diversity on invertebrate herbivory in experimental grassland. *Oecologia*, *147*(3), 489–500. https://doi.org/10.1007/s00442-005-0281-3

Simms, E. L., & Rausher, M. D. (1987). Costs and benefits of plant resistance to herbivory. *The American Naturalist*, *130*(4), 570–581.

Speed, M. P., Fenton, A., Jones, M. G., Ruxton, G. D., & Brockhurst, M. A. (2015). Coevolution can explain defensive secondary metabolite diversity in plants. *New Phytologist*, *208*(4), 1251–1263. https://doi.org/10.1111/nph.13560

Sporer, T., Körnig, J., Wielsch, N., Gebauer-Jung, S., Reichelt, M., Hupfer, Y., & Beran, F. (2021). Hijacking the mustard-oil bomb: How a glucosinolate-sequestering flea beetle copes with plant myrosinases. *Frontiers in Plant Science*, *12*, 645030. https://doi.org/10.3389/fpls.2021.645030

Strauss, S. Y., Cacho, N. I., Schwartz, M. W., Schwartz, A. C., & Burns, K. C. (2015). Apparency revisited. *Entomologia Experimentalis et Applicata*, *157*(1), 74–85. https://doi.org/10.1111/eea.12347

Strauss, S. Y., Rudgers, J. A., Lau, J. A., & Irwin, R. E. (2002). Direct and ecological costs of resistance to herbivory. *Trends in Ecology & Evolution*, *17*(6), 278–285. https://doi.org/10.1016/S0169-5347(02)02483-7

Wang, K., Rusman, Q., van Bergen, E., & Züst, T. (2025). *Effects of dual chemical defences on herbivory: Leaf damage and herbivore abundance in* Erysimum cheiranthoides *are negatively associated with cardenolides, but not glucosinolates.*

Wang, K., & Züst, T. (2025). Within□plant variation in chemical defence of *Erysimum cheiranthoides* does not explain *Plutella xylostella* feeding preference. *Plant Biology*, plb.13777. https://doi.org/10.1111/plb.13777

War, A. R., Paulraj, M. G., Ahmad, T., Buhroo, A. A., Hussain, B., Ignacimuthu, S., & Sharma, H. C. (2012). Mechanisms of plant defense against insect herbivores. *Plant Signaling & Behavior*, *7*(10), 1306–1320. https://doi.org/10.4161/psb.21663

Wittstock, U., Agerbirk, N., Stauber, E. J., Olsen, C. E., Hippler, M., Mitchell-Olds, T., Gershenzon, J., & Vogel, H. (2004). Successful herbivore attack due to metabolic diversion of a plant chemical defense. *Proceedings of the National Academy of Sciences of the United States of America*, *101*(14), 4859–4864. https://doi.org/10.1073/pnas.0308007101

Wood, S. N., Pya, N., & Säfken, B. (2016). Smoothing parameter and model selection for general smooth models. *Journal of the American Statistical Association*, *111*(516), 1548–1563. https://doi.org/10.1080/01621459.2016.1180986

Younkin, G. C., Alani, M. L., Páez□Capador, A., Fischer, H. D., Mirzaei, M., Hastings, A. P., Agrawal, A. A., & Jander, G. (2024). Cardiac glycosides protect wormseed wallflower (*Erysimum cheiranthoides*) against some, but not all, glucosinolate□adapted herbivores. *New Phytologist*, *242*(6), 2719–2733. https://doi.org/10.1111/nph.19534

Zalucki, J. M., Heckel, D. G., Wang, P., Kuwar, S., Vassão, D. G., Perkins, L., & Zalucki, M. P. (2021). A generalist feeding on Brassicaceae: It does not get any better with selection. *Plants*, *10*(5), 954. https://doi.org/10.3390/plants10050954

Zangerl, A. R., Hamilton, J. G., Miller, T. J., Crofts, A. R., Oxborough, K., Berenbaum, M. R., & de Lucia, E. H. (2002). Impact of folivory on photosynthesis is greater than the sum of its holes. *Proceedings of the National Academy of Sciences of the United States of America*, *99*(2), 1088–1091. https://doi.org/10.1073/pnas.022647099

Züst, T., & Agrawal, A. A. (2017). Trade-offs between plant growth and defense against insect herbivory: An emerging mechanistic synthesis. *Annual Review of Plant Biology*, *68*(1), 513–534. https://doi.org/10.1146/annurev-arplant-042916-040856

Züst, T., Heichinger, C., Grossniklaus, U., Harrington, R., Kliebenstein, D., & Turnbull, L. (2012). Natural enemies drive geographic variation in plant defenses. *Science*, *338*(6103), 116–119. https://doi.org/10.1126/science.1226397

Züst, T., Joseph, B., Shimizu, K. K., Kliebenstein, D. J., & Turnbull, L. A. (2011). Using knockout mutants to reveal the growth costs of defensive traits. *Proceedings of the Royal Society B: Biological Sciences*, *278*(1718), 2598–2603. https://doi.org/10.1098/rspb.2010.2475

Züst, T., Rasmann, S., & Agrawal, A. A. (2015). Growth-defense tradeoffs for two major anti-herbivore traits of the common milkweed *Asclepias syriaca*. *Oikos*, *124*(10), 1404–1415. https://doi.org/10.1111/oik.02075

Züst, T., Strickler, S. R., Powell, A. F., Mabry, M. E., An, H., Mirzaei, M., York, T., Holland, C. K., Kumar, P., Erb, M., Petschenka, G., Gómez, J.-M., Perfectti, F., Müller, C., Pires, J. C., Mueller, L. A., & Jander, G. (2020). Independent evolution of ancestral and novel defenses in a genus of toxic plants (*Erysimum*, Brassicaceae). *eLife*, *9*, e51712. https://doi.org/10.7554/eLife.51712

Supplementary Materials

Supplementary Methods

1. Analysis of herbivore community composition

We first analysed total herbivore abundance using separate negative binomial generalized linear mixed effects models (GLMMs, function *glmmTMB* in R package glmmTMB; Brooks et al., 2017) for each year. For each herbivore species, counts were summed per plant across six observation dates and modelled with fixed effects of plant species, herbivore species, and their interaction, with random intercepts included for plant genotype and plant identity. For the 2023 experiment, we excluded the competition treatment due to incomplete observations, but we included the insecticide treatment as an additional fixed effects with all interactions. Significance of fixed effects was assessed using Type III Wald X^2 tests implemented in the function *Anova* (R package car). Post hoc pairwise comparisons were performed using function *emmeans* (R package emmeans) to test for plant-species differences under ambient conditions and insecticide effects within each plant species.

Next, we compared herbivore community composition for *R. nigrum* and *E. cheiranthoides* across years and among treatments (for the 2023 experiment) using multivariate analysis of field observation data. For comparisons between years, we excluded the competition and insecticide treatments of the 2023 experiment and summed observations from week 4 and 5 for each remaining plant (corresponding to peak herbivore abundance in both years). For comparison among treatments within in the 2023 experiment, we used data from week 4 only, as later weeks lacked observations for the competition treatment. For both reduced datasets, we calculated Bray-Curtis dissimilarity matrices from square-root-transformed herbivore counts and tested for differences in community composition using PERMANOVA (function *adonis2*, R package vegan; Oksanen et al. 2025). Homogeneity of multivariate dispersion was evaluated using function *permutest* applied to *betadisper* results, and non-metric multidimensional scaling (NMDS, function *metaMDS*) was used to visualize patterns in community composition (all in R package vegan).

2. Prediction of total leaf number from size measurements

Total leaf number was recorded only for a subset of plants in 2023. To obtain leaf number estimates for all plants, we used a two-stage predictive modelling approach. All models were trained separately for *R. nigrum* and *E. cheiranthoides* because the two species differ strongly in morphology and leaf numbers. For *R. nigrum*, we used candidate predictors of observation week, plant height, and plant width, including all pairwise interactions. For *E. cheiranthoides*, branch number and its pairwise interactions were additionally included as predictors because this species was frequently branched. Main effects and interactions were encoded using species-specific model-matrix representations, ensuring consistent predictor structure across all models within each species.

We used Poisson LASSO (least absolute shrinkage and selection operator) regression to identify a parsimonious set of predictors (function *cv.glmnet* in R package glmnet; Friedman et al. 2010). For each species, we fitted a cross-validated model using the subset of plants with observed total leaf number. To obtain a stable and conservative predictor selection, we performed 200 non-parametric bootstrap resamples for each species, refitting the LASSO model to each bootstrap sample. For every model refit, we recorded all predictors with non-zero coefficients at the regularization value *lambda.min*. Predictors retained in ≥ 70% of all bootstrap replicates were considered stable and used for the final model. This 'stability selection' step reduces sensitivity to sampling variation and guards against overfitting.

Because count data often show overdispersion relative to a Poisson distribution, we re-fitted the final predictive model for each species using a negative binomial generalized linear model (function *glm.nb* in R package MASS, Venables & Ripley 2002). Each negative binomial model included only the predictors identified through stability selection. These final models were then used to predict total leaf number for all plants lacking observations.

For subsequent analyses of herbivore damage, we always used the observed leaf number when available. For plants lacking observations, we used the predicted leaf number unless the predicted value was lower than the total number of damaged leaves, in which case the number of damaged leaves was used as the total leaf count. This ensures biological plausibility and prevents damage estimates from exceeding total leaf number.

3. Plant height growth modelling

Plant height was recorded as a simple measure of plant size during damage assessments in 2022 (weeks 3, 6, and 9), and weekly in 2023. In 2022, height was measured from the root base to the tallest point of a plant, including leaves. However, this approach introduced variability due to differences in leaf size and leaf angle. To obtain a more standardized measure of structural growth, we recorded plant height in 2023 as stem height, measured from the root base to the apical meristem.

We modelled plant height growth using a four-parameter logistic function of the form

$$H = H_0 + \frac{K - H_0}{1 + e^{\left(-r(t - t_{mid})\right)}} \qquad \text{[eqn 1]},$$

where plant height H at time t is a function of the initial plant height H_0 (i.e., height at transplanting), the asymptotic maximum height K, the growth rate r, and the time of the inflection point t_{mid} (i.e., the time when height is halfway between H_0 and K). We fitted equation 1 to plant height data using the *nlme* function from the R package nlme, treating plant identity as random effect to account for repeated measures of individual plants.

As we only recorded height three times in the 2022 field experiment, our ability to estimate all four model parameters was limited. We therefore fixed parameters t_{mid} and r at species-specific values, using an iterative process. For each species, we first set r = 0.1 and fitted models across a

range of t_{mid} values (20-60 days). We compared models using AIC and selected the value of t_{mid} that minimized AIC. Holding t_{mid} constant at this optimal value, we then repeated the procedure across a range of r values (0.05-0.5) to identify optimal species-specific values of r that minimized AIC. Using these optimal values as fixed parameters, we refitted the model to the full data to estimate the remaining two parameters, specifying fixed effects of plant species for both H_0 and K, and sequentially removing non-significant model terms.

For the 2023 field experiment, weekly recordings resulted in up to nine height measurements per plant. We removed plants with fewer than five observations (e.g., due to mortality), which allowed us to estimate all four parameters directly from the data. We also excluded plants from the competition treatment as we stopped recording their heights in the second half of the experiment. Fixed effects of plant species, insecticide treatment, and their interaction were included for parameters K, t_{mid}, and r. For H_0, we included only plant species as a fixed effect, as insecticide treatment was applied after transplanting and therefore could not influence initial height. Starting from a full model, we simplified the model by sequentially removing non-significant terms.

To compare growth dynamics between species and insecticide treatment over time, we calculated the absolute growth rate (AGR) from the derivative of equation 1:

$$AGR = \frac{r(K-H_0)e^{\left(-r(t-t_{mid})\right)}}{\left(1+e^{\left(-r(t-t_{mid})\right)}\right)^2} \qquad \text{[eqn 2].}$$

We calculated AGR for the midpoints of the first (weeks 3-6) and second (weeks 6-9) growth interval in both years. For each set of AGR estimates, we generated 95% population prediction intervals by drawing random values from the sampling distribution of each of the estimated parameters (Bolker, 2008).

4. Leaf traits

Leaves from subsets of plants in the 2022 field experiment were harvested in weeks 4, 7, and 10 (one week after damage assessments) to assess temporal changes in plant nutritional quality. Each plant was only sampled once: plants from blocks 1-3 were sampled in week 4, blocks 4-6 in week 7, and blocks 7-10 in week 10. For each sampling, we removed 5-10 leaves from *R. nigrum* or 10-20 leaves from *E. cheiranthoides*, selecting and pooling leaves from the top, middle, and lower parts of each plant. Leaves from the same individual were wrapped together in aluminium foil and immediately placed on dry ice. Frozen samples were transported to the laboratory and stored at -80 °C before freeze-drying under vacuum for 48 h.

All *R. nigrum* samples were included in the analyses, whereas for *E. cheiranthoides* we analysed a random subset that also included genotypes excluded from the main analyses. For each selected plant, dried leaves were homogenized, and two aliquots of 10 mg were weighed into separate 2 mL screw-

cap plastic tubes (Avantor, USA). One aliquot was used for determination of total protein content, and the other was used for determination of sugar and starch content.

4.1 Total protein content

Total protein content of leaves was determined following Clissold et al. (2006). Briefly, 10 mg of ground leaf material was extracted twice using a total volume of 0.8 mL 0.1M NaOH. Samples were sonicated for 30 minutes, heated at 90 °C for 15 min, and centrifuged. Supernatants were pooled and neutralized with 6 M HCl. We precipitated proteins by adding 90 µL trichloroacetic acid solution (100% w/v, Sigma-Aldrich, Switzerland), followed by centrifugation and washing of the protein pellet with cold acetone. Dried pellets were resuspended in 1 mL of 0.1M NaOH, diluted 1:20 with water, and 50 µL of this solution was assayed photometrically using 200 µL QuickStart™ Bradford Dye (BioRad, Switzerland). Absorbance was read at 595 nm on a microplate reader. Each sample was assayed in triplicate, and protein concentrations were calculated using an Immunoglobuline G (Sigma-Aldrich, Switzerland) standard curve (0-12 µg protein per assay).

4.2 Soluble sugars and starch content

Soluble sugars were quantified following Machado et al. (2013). Ground plant material was extracted with 0.5 mL 80% ethanol, and re-extracted twice using 0.5 mL 80% ethanol. For each extraction, samples were vortexed, heated at 78 °C for 15 min, and centrifuged. Supernatants were pooled, and 25 µL of each extract were used for sequential determination of glucose, fructose, and sucrose using the enzymatic assay of Velterop & Vos (2001). Briefly, glucose was converted to glucose-6-phosphate by hexokinase (Roche, Switzerland) in the presence of ATP (Sigma-Aldrich, Switzerland), and further converted to 6-phosphogluconate by glucose-6-P-dehydrogenase (Roche, Switzerland) with $NADP^+$ (Sigma-Aldrich, Switzerland). The resulting NADPH was quantified photometrically at 340 nm. After readings stabilized, phosphoglucoisomerase (Roche, Switzerland) was added to convert fructose to glucose, and absorbance was read again. Finally, we added invertase (Sigma-Aldrich, Switzerland) to convert sucrose into glucose and fructose, and absorbance was read a third time. All reactions were carried out in 50 mM HEPES buffer (pH 7, with 5 mM $MgCl_2$). Each sample was run in triplicate, and sugars were quantified relative to a glucose standard curve (0-2 mM).

Starch content was determined from the pellet remaining after sugar extraction, following Smith & Zeeman (2006). We added 1 mL of water to each pellet and diluted 100 µL of this suspension with 500 µL water. Dilute suspensions were autoclaved for 1 h cooled to 37 °C. We then added 500 µL of an enzyme solution containing 50 mM sodium-acetate buffer (pH 5.5), amyloglucosidase (Roche, Switzerland) and α-amylase (Sigma-Aldrich, Switzerland). Samples were incubated overnight at 37 °C, and glucose equivalents were quantified in in 25 µL of supernatant using the same enzymatic assay as above.

4.3 Trichome density and length

Trichomes were quantified on separate greenhouse-grown plants of *R. nigrum* and *E. cheiranthoides* (only using one genotype). Plants were germinated and grown as in the field experiments and maintained in the greenhouse for four weeks. We then measured trichome densities and lengths on both sides of single leaves from six plants per species. High-resolution images were acquired using an Emspira 3 digital microscope (Leica Microsystems, Switzerland, Figure S8a-d). Trichomes were counted within defined areas using ImageJ (Schneider et al. 2012). For three leaves per species and leaf side, we also measured the lengths of eight trichomes using ImageJ.

5. Herbivore choice assays

To complement field observations with controlled tests of herbivore preference, compared feeding choices of four laboratory-reared herbivores between *R. nigrum* and *E. cheiranthoides* (only using one genotype). All used herbivores specialize on Brassicaceae and tolerate glucosinolates, but differ in their natural association with *E. cheiranthoides*. The turnip sawfly *Athalia rosae* (Hymenoptera: Tenthredinidae) has no known association with *E. cheiranthoides* but feeds on other Brassicaceae plants as larvae and sequesters glucosinolates from its host plants (Müller & Wittstock, 2005). The cabbage white butterfly *Pieris rapae* (Lepidoptera: Pieridae) actively avoids *E. cheiranthoides* (Sachdev-Gupta et al., 1993; Younkin et al., 2024) but its caterpillars feed on other Brassicaceae plants by detoxifying activated glucosinolates enzymatically (Wittstock et al., 2004). The diamondback moth *Plutella xylostella* (Lepidoptera: Plutellidae) is occasionally found feeding on *E. cheiranthoides* (Mertens et al., 2021; observations in current study) and its caterpillars enzymatically degrade glucosinolates prior to their activation (Ratzka et al., 2002), while the cardenolide coping mechanism remains unknown. Finally, the red cabbage bug *Eurydema ornata* (Hemiptera: Pentatomidae) is frequently found feeding on *E. cheiranthoides* and other *Erysimum* species both as adults and nymphs (Goméz, 2005; observations in current study). Individuals sequester glucosinolates from their host plant (Aliabadi et al., 2002), but again the cardenolide coping mechanism for this species remains unknown.

Individuals of *A. rosae* were kindly provided by Prof. Caroline Müller, University of Bielefeld, and had been maintained as a laboratory rearing colony on *Sinapis arvensis*. Newly eclosed, unmated females were left to oviposit on *Brassica rapa* plants (Wisconsin Fast Plants^{TM}, Caroline Biological Supply Co., Burlington VA, USA), and the developing male larvae were used for choice assays 5 days after hatching. Individuals of *P. rapae* were kindly provided by the group of Prof. Florian Schiestl, University of Zürich. Adults had originally been collected from multiple locations in Switzerland and were maintained in a panmictic laboratory rearing colony using *Brassica rapa* plants as oviposition substrate and leaves of savoy cabbage (*Brassica oleracea* var. *sabauda*) as caterpillar food. We placed fresh *B. rapa* plants in an adult oviposition cage for 24 hours, after which larvae were left to develop on the oviposition plant for 10 days before use in choice assays (early L2 stage).

For *P. xylostella* we used a strain from a long-term rearing on a wheat germ-based artificial diet (Frontier Agricultural Sciences, Delaware, USA), originally provided by Syngenta Crop Protection AG, Stein, Switzerland. For choice assays, newly laid eggs on sheets of parafilm were placed in cups of fresh diet and left to develop for 11 days (late L2 stage). We originally collected adults of *E. ornata* from a population in Valais, Switzerland (46.312970° N, 7.675072° E, predominantly collected on *Isatis tinctoria*), and maintained a continuous laboratory rearing population on a diet of savoy cabbage leaves and young *B. rapa* plants, with yearly introductions of new individuals from the same wild population to maintain genetic diversity. For choice assays, we used mature adults (>3 days after final molt) out of the rearing population.

Choice assays were set up in petri dishes (5 cm diameter) containing a thin layer of 3% agar, with 12 replicates per herbivore species. Each petri dish contained paired leaf discs (7.6 mm diameter), one from *R. nigrum* and one from *E. cheiranthoides* (4-week old greenhouse plants). A single larva (for *A. rosae*, *P. rapae*, *P. xylostella*) or adult (for *E. ornata*) was released at dish centre. Larvae (leaf chewers) were allowed to feed for 6 h, whereas *E. ornata* (cell-content feeder) fed for 24 h. Remaining leaf discs were scanned using a CanoScan LiDE 220 scanner, and remaining leaf area was quantified in ImageJ. Consumed area was calculated by subtracting remaining leaf areas from the area of an intact leaf disc (45.36 mm^2).

Consumed leaf areas were analysed with a linear mixed-effects model including plant species, herbivore species, and their interaction as fixed effects, and Petri dish ID as a random effect to account for paired discs. Species-specific preferences were then tested using pairwise contrasts (function *emmeans*).

Supplementary Results

Herbivore community composition

We compared herbivore community composition between years by focused on individual plants under ambient herbivore conditions and summed observations from weeks 4 and 5, representing peak abundance in both years. Using PERMANOVA, we found a significant interaction between plant species and year ($F_{1,408} = 10.32$, $p < 0.001$), although group dispersion also differed substantially for both factors (permutation tests on *betadisper*, $p < 0.001$).

To compare composition among the factorial combination of competition and insecticide treatments in 2023, we analysed observations from week 4, corresponding to high abundance and complete sampling across all treatments. We detected a marginally significant three-way interaction between plant species, insecticide treatment, and competition ($F_{1,283} = 2.49$, $p = 0.070$), thus we analysed plants separately. For *R. nigrum*, community composition differed by insecticide ($F_{1,85} = 22.45$, $p < 0.001$) but not by competition ($F_{1,85} = 1.28$, $p = 0.274$), and group dispersion was homogeneous across treatment (permutation tests, insecticide: $p = 0.680$, competition: $p = 0.119$; Supplementary Figure S2a). In contrast, community composition on *E. cheiranthoides* differed

significantly by both insecticide ($F_{1,200} = 79.04$, $p < 0.001$) and competition ($F_{1,200} = 21.19$, $p < 0.001$), but group dispersion also differed for the competition treatment (permutation tests, insecticide: $p = 0.420$, competition: $p < 0.001$; Supplementary Figure S2b).

Species differences in plant traits

In the 2022 field experiment, we quantified nutritional traits that may influence herbivore preference. Across three sampling points, *R. nigrum* leaves contained significantly higher concentrations of soluble glucose and fructose (Fig. S7a-b), whereas *E. cheiranthoides* contained higher levels of sucrose (Fig. S7c). Digestible starch content did not differ between species for most of the experiment, except at the final sampling, when starch had declined in both species but more strongly in *E. cheiranthoides* (Fig. S7d). Total hydrolysable protein content differed only at later time points, with *R. nigrum* containing up to 60% more protein per unit dry mass.

Trichomes differed markedly between the two plant species, with *R. nigrum* producing long, unbranched trichomes (Figure S8a-b), whereas *E. cheiranthoides* had smaller, medifixed stellate trichomes (Figure S8c-d). Trichome density on *R. nigrum* was lowest on the upper (adaxial) surface (0.04 ± 0.01 trichomes mm^{-2}; mean ± 1 SE) and slightly higher on the lower (abaxial) surface (0.21 ± 0.07 trichomes mm^{-2}), where trichomes were predominantly located along veins. In contrast, *E. cheiranthoides* had very high trichome densities on both surfaces (adaxial: 8.84 ± 0.61 trichomes mm^{-2}; abaxial: 7.50 ± 0.52 trichomes mm^{-2}). Although trichome density and morphology may vary with plant age and environment, these measurements nonetheless provide a useful reference for the relative differences between *R. nigrum* and *E. cheiranthoides*.

Supplementary References

Aliabadi, A., Renwick, J. A. A., Whitman, D. W. (2002). Sequestration of glucosinolates by harlequin bug *Murgantia histrionica*. *Journal of Chemical Ecology 28*, 1749-1762.

Bolker, B. M. (2008). Ecological Models and Data in R. Princeton University Press.

Brooks, M., E., Kristensen, K., Benthem, K., J. ,van, Magnusson, A., Berg, C., W., Nielsen, A., Skaug, H., J., Mächler, M., & Bolker, B., M. (2017). glmmTMB balances speed and flexibility among packages for zero-inflated generalized linear mixed modeling. The R Journal, 9(2), 378. https://doi.org/10.32614/RJ-2017-066

Clissold, F. J., Sanson, G. D., & Read, J. (2006). The paradoxical effects of nutrient ratios and supply rates on an outbreaking insect herbivore, the Australian plague locust. *Journal of Animal Ecology 75*, 1000-1013.

Friedman, J., Hastie, T., & Tibshirani, R. (2010). Regularization Paths for Generalized Linear Models via Coordinate Descent. *Journal of Statistical Software* 33, 1-22.

Machado, R. A. R., Ferrieri, A. P., Robert, C. A. M., Glauser, G., Kallenbach, M., Baldwin, I. T., & Erb, M. (2013). Leaf-herbivore attack reduces carbon reserves and regrowth from the roots via jasmonate and auxin signaling. *New Phytologist 200*, 1234-1246.

Müller, C. & Wittstock, U. (2005). Uptake and turn-over of glucosinolates sequestered in the sawfly *Athalia rosae*. *Insect Biochemistry and Molecular Biology* 35, 1189-1198.

Oksanen, J., Simpson, G. L., Blanchet, F. G., Kindt, R., Legendre, P., Minchin, P., O'Hara, R. B., Solymos, P., Stevens, M. H. H., Szoecs, E., Wagner, H., Barbour, M., Bedward, M., Bolker, B., Borcard, D., Borman, T., Carvalho, G., Chirico, M., De Caceres, M., … Weedon, J. (2025). *vegan: Community ecology package* [Computer software].

Schneider C.A., Rasband W.S., Eliceiri K.W. (2012). NIH Image to ImageJ: 25 years of image analysis. *Nature Methods 9*, 671–675.

Smith, A. M., & Zeeman, S. C. (2006). Quantification of starch in plant tissues. *Nature Protocols 1*, 1342–1345.

Velterop, J. S., & Vos, F. (2001). A rapid and inexpensive microplate assay for the enzymatic determination of glucose, fructose, sucrose, L-malate and citrate in tomato (*Lycopersicon esculentum*) extracts and in orange juice. *Phytochemical Analysis 12*, 299–304.

Venables, W. N., & Ripley, B. D. (2002). Modern applied statistics with S. Fourth Edition. Springer, New York.

Table S1. Mean (± 1 SE) numbers of herbivores per plant observed sitting or feeding on *R. nigrum* and *E. cheiranthoides* in the 2022 field experiment, summed across six observation dates. Values are back-transformed model predictions from a negative binomial generalized linear mixed-effects model of herbivore counts as a function of plant species and herbivore species. Numbers in parentheses in the table header indicate the number of replicate plants per species. Pairwise linear contrasts were used to test for differences between plants for each herbivore species (*Rha vs. Ery*). Bold values highlight significant contrasts. Flea beetles, large flea beetles, weevils, and leaf hoppers refer to taxonomically complex groups that were not identified to species level in the field.

Herbivore	Scientific name	Order	Stage	*R. nigrum* (n = 28)	*E. cheiranthoides* (n = 62)	Pairwise contrast *Rha vs. Ery*
flea beetle		Coleoptera	adult	24.10 ± 4.50	1.61 ± 0.26	**z-ratio = 11.10, p < 0.001**
pollen beetle	*Brassicogethes aeneus*	Coleoptera	adult	88.20 ± 16.00	4.95 ± 0.68	**z-ratio = 12.70, p < 0.001**
weevil		Coleoptera	adult	3.94 ± 0.69	0.81 ± 0.13	**z-ratio = 6.22, p < 0.001**
leaf miner	*Phytomyza sp.*	Diptera	juvenile	0.34 ± 0.12	0.04 ± 0.03	**z-ratio = 2.96, p = 0.003**
aphid		Hemiptera	adult/juvenile	6.92 ± 1.39	0.66 ± 0.13	**z-ratio = 8.35, p < 0.001**
cabbage whitefly	*Aleyrodes sp.*	Hemiptera	adult	7.74 ± 1.52	0.29 ± 0.07	**z-ratio = 10.2, p < 0.001**
leaf hopper		Hemiptera	adult	0.06 ± 0.05	0.06 ± 0.03	z-ratio = 0.07, p = 0.943
crucifer shield bug	*Eurydema sp.*	Heteroptera	adult/juvenile	0.64 ± 0.19	0.70 ± 0.14	z-ratio = -0.29, p = 0.775
plant bug	*Lygus sp.*	Heteroptera	adult/juvenile	5.12 ± 1.02	0.83 ± 0.15	**z-ratio = 6.68, p < 0.001**
potato capsid	*Closterotomus norwegicus*	Heteroptera	adult	0.16 ± 0.08	0.07 ± 0.03	z-ratio = 1.13, p = 0.260
diamondback moth	*Plutella xylostella*	Lepidoptera	adult/juvenile	1.70 ± 0.40	0.59 ± 0.12	**z-ratio = 3.46, p < 0.001**

Table S2. Mean (± 1 SE) numbers of herbivores per plant observed sitting or feeding on individual *R. nigrum* and *E. cheiranthoides* in the 2023 field experiment (excluding plants of the competition treatment), summed across six observation dates. Values are back-transformed model predictions from a negative binomial generalized linear mixed-effects model of herbivore counts as a function of plant species, herbivore species, and insecticide treatment. Numbers in parentheses in the table header indicate the number of replicate plants per species and treatment. Pairwise linear contrasts were used to test for differences between plant species under ambient conditions (*Rha vs. Ery | Ambient)*, and for the effects of insecticide treatment within *R. nigrum* (*Ambient vs. Sprayed | Rha*) and *E. cheiranthoides* (*Ambient vs. Sprayed | Ery*). Bold values highlight significant contrasts, and colours additionally highlight significant decreases (blue) or increases (red) in mean numbers for each contrast. Leaf miners were never observed on *R. nigrum* in 2023 and could not be analysed in this model.

Herbivore	*R. nigrum* (n = 9) *Ambient*	*E. cheiranthoides* (n =74) *Ambient*	Pairwise contrast *Rha vs. Ery | Ambient*	*R. nigrum* (n = 6) *Sprayed*	Pairwise contrast *Ambient vs. Sprayed | Rha*	*E. cheiranthoides* (n = 63) *Sprayed*	Pairwise contrast *Ambient vs. Sprayed | Ery*
flea beetle	143.00 ± 40.80	19.80 ± 1.96	**z-ratio = 6.58, p < 0.001**	224.00± 67.00	z-ratio = -1.19, p = 0.232	3.42 ± 0.41	**z-ratio = 12.10, p < 0.001**
pollen beetle	15.30 ± 4.57	9.46 ± 0.98	z-ratio = 1.51, p = 0.130	94.50 ± 28.50	**z-ratio = -4.72, p < 0.001**	11.50 ± 1.23	z-ratio = -1.44, p = 0.151
weevil	7.76 ± 2.41	1.32 ± 0.18	**z-ratio = 5.21, p < 0.001**	28.9 ± 8.91	**z-ratio = -3.29, p = 0.001**	1.73 ± 0.24	z-ratio = -1.46, p = 0.144
leaf miner	n/a	n/a	n/a	n/a	n/a	n/a	n/a
aphid	95.80 ± 27.90	15.60 ± 1.59	**z-ratio = 5.89, p < 0.001**	417.00 ± 125.00	**z-ratio = -3.88, p < 0.001**	86.80 ± 8.75	**z-ratio = -13.10, p < 0.001**
cabbage whitefly	0.23 ± 0.18	0.45 ± 0.09	z-ratio = -0.86, p = 0.391	8.81 ± 2.92	**z-ratio = -4.47, p < 0.001**	0.31 ± 0.08	z-ratio = 1.20, p = 0.229
leaf hopper	0.12 ± 0.12	0.07 ± 0.03	z-ratio = 0.49, p = 0.622	0	z-ratio = 0.01, p = 0.995	0.03 ± 0.02	z-ratio = 0.96, p = 0.338
crucifer shield bug	1.19 ± 0.51	1.58 ± 0.21	z-ratio = -0.63, p = 0.532	0.27 ± 0.21	z-ratio = 1.71, p = 0.087	0.91 ± 0.15	**z-ratio = 2.69, p = 0.007**
plant bug	1.39 ± 0.56	0.15 ± 0.05	**z-ratio = 4.38, p < 0.001**	2.17 ± 0.86	z-ratio = -0.83, p = 0.407	0.25 ± 0.07	z-ratio = -1.35, p = 0.177
potato capsid	1.44 ± 0.58	0.09 ± 0.04	**z-ratio = 4.89, p < 0.001**	1.07 ± 0.50	z-ratio = 0.50, p = 0.621	0.03 ± 0.02	**z-ratio = 1.40, p = 0.0161**
diamondback moth	0.12 ± 0.12	0.34 ± 0.08	z-ratio = -1.00, p = 0.317	3.86 ± 1.37	**z-ratio = -3.21, p = 0.001**	1.07 ± 0.15	**z-ratio = -4.10, p < 0.001**

Table S3. Generalized additive model (GAM) results for temporal dynamics in herbivore presence in the 2022 and 2023 field experiments. a) For 2022, separate binomial GAMs were fitted to presence-absence data of each herbivore with a fixed effect of plant species. Nested models with either a global temporal smoother ('day'), plant-specific smoothers ('day by plant') were compared based on AIC, retaining the simpler model unless ΔAIC >2. The number smoother nodes (*k*) were fixed to 5 for each model, and significance of fixed effect was assessed using Type III Wald chisquare tests on explained deviance. b) For 2023, equivalent GAMs were fitted with fixed effects of plant species and insecticide treatment (plants of the competition treatment were excluded). Models with additive *vs.* interactive fixed effects were compared based on AIC, followed by comparison of alternative smoother structures ('day', 'day by plant', 'day by insecticide', 'day by plant × insecticide'). No model could be fitted for crucifer shield bugs on insecticide-treated plants due to insufficient observations.

a) 2022 field experiment

Herbivore	Plant		Smoother
aphids	**df = 1, X^2 = 36.77**	**p < 0.001**	day
cabbage whitefly	**df = 1, X^2 = 39.25**	**p < 0.001**	day
crucifer shield bug	df = 1, X^2 = 1.10	p = 0.295	day
diamondback moth	**df = 1, X^2 = 19.66**	**p < 0.001**	day
flea beetle	**df = 1, X^2 = 5.78**	**p = 0.016**	day by plant
plant bug	df = 1, X^2 = 2.16	p = 0.142	day by plant
pollen beetle	**df = 1, X^2 = 37.86**	**p < 0.001**	day by plant
weevil	**df = 1, X^2 = 21.37**	**p < 0.001**	day by plant

b) 2023 field experiment

Herbivore	Plant		Insecticide		Plant × Insecticide		Smoother
aphids	df = 1, X^2 = 0.05	p = 0.829	**df = 1, X^2 = 18.32**	**p < 0.001**	df = 1, X^2 = 2.20	p = 0.138	day by insecticide
cabbage whitefly	df = 1, X^2 = 0.95	p = 0.331	**df = 1, X^2 = 5.90**	**p = 0.015**	**df = 1, X^2 = 6.25**	**p = 0.013**	day
crucifer shield bug	df = 1, X^2 = 1.38	p = 0.241	n/a	n/a	n/a	n/a	day by plant
diamondback moth	df = 1, X^2 = 0.96	p = 0.327	**df = 1, X^2 = 8.37**	**p = 0.004**	**df = 1, X^2 = 4.63**	**p = 0.031**	day
flea beetle	**df = 1, X^2 = 27.51**	**p < 0.001**	**df = 1, X^2 = 46.22**	**p < 0.001**	n.s.	n.s.	day by insecticide
plant bug	df = 1, X^2 = 0.04	p = 0.834	df = 1, X^2 = 3.17	p = 0.075	n.s.	n.s.	day by plant
pollen beetle	**df = 1, X^2 = 6.34**	**p = 0.012**	**df = 1, X^2 = 5.72**	**p = 0.017**	**df = 1, X^2 = 5.61**	**p = 0.018**	day by plant
weevil	**df = 1, X^2 = 11.24**	**p < 0.001**	df = 1, X^2 = 3.04	p = 0.081	df = 1, X^2 = 1.19	p = 0.276	day

Table S4. Generalized additive model (GAM) results for temporal dynamics in herbivore abundance in the 2022 and 2023 field experiments. a) For 2022, separate negative binomial GAMs were fitted to count data of each herbivore after weeks with zero observations were excluded. Models included fixed effect of plant species, and nested models with a global temporal smoother ('day') or a plant-specific smoothers ('day by plant') were compared based on AIC, retaining the simpler model unless ΔAIC >2. The number smoother nodes (*k*) was adjusted for each model according to the number of weeks in which herbivores were observed. Significance of fixed effect was assessed using Type III Wald chisquare tests on explained deviance, and intraclass correlation coefficients (ICC) were calculated to evaluate plant genotype effects. No model could be fitted for cabbage whiteflies due to insufficient observations. b) For 2023, equivalent GAMs were fitted with fixed effects of plant species and insecticide treatment (plants of the competition treatment were excluded). Models with additive *vs.* interactive fixed effects were compared based on AIC, followed by comparison of alternative smoother structures. No model could be fitted for crucifer shield bugs on insecticide-treated plants due to insufficient observations.

a) 2022 field experiment

Herbivore	Plant		Smoother	k	ICC Genotype
aphids	**df = 1, X^2 = 68.47**	**p < 0.001**	day by plant	5	0.0000
crucifer shield bug	df = 1, X^2 = 0.11	p = 0.740	day	3	0.0000
diamondback moth	**df = 1, X^2 = 26.36**	**p < 0.001**	day	3	0.0000
flea beetle	**df = 1, X^2 = 35.96**	**p < 0.001**	day by plant	5	0.0740
plant bug	**df = 1, X^2 = 26.89**	**p < 0.001**	day by plant	3	0.0464
pollen beetle	**df = 1, X^2 = 171.14**	**p < 0.001**	day by plant	3	0.0208
weevil	**df = 1, X^2 = 19.06**	**p < 0.001**	day by plant	3	0.0901

b) 2023 field experiment

Herbivore	Plant		Insecticide		Plant × Insecticide		Smoother	k	ICC Genotype
aphids	**df = 1, X^2 = 13.62**	**p < 0.001**	**df = 1, X^2 = 78.31**	**p < 0.001**	n.s.	n.s.	day by plant × insecticide	5	0.0636
cabbage whitefly	df = 1, X^2 = 0.44	p = 0.509	**df = 1, X^2 = 12.58**	**p < 0.001**	**df = 1, X^2 = 15.10**	**p < 0.001**	day by insecticide	3	0.0277
crucifer shield bug	df = 1, X^2 = 0.70	p = 0.403	n/a	n/a	n/a	n/a	day by plant	3	0.1378
diamondback moth	df = 1, X^2 = 1.01	p = 0.314	**df = 1, X^2 = 9.35**	**p = 0.002**	**df = 1, X^2 = 4.57**	**p = 0.032**	day	4	0.0290
flea beetle	**df = 1, X^2 = 126.89**	**p < 0.001**	df = 1, X^2 = 0.09	p = 0.769	**df = 1, X^2 = 37.74**	**p < 0.001**	day	5	0.0000
plant bug	**df = 1, X^2 = 39.57**	**p < 0.001**	df = 1, X^2 = 2.24	p = 0.134	n.s.	n.s.	day by plant	3	0.0000
pollen beetle	df = 1, X^2 = 0.00	p = 0.987	**df = 1, X^2 = 18.46**	**p < 0.001**	**df = 1, X^2 = 5.61**	**p < 0.001**	day by plant × insecticide	3	0.2579
weevil	**df = 1, X^2 = 23.08**	**p < 0.001**	**df = 1, X^2 = 6.78**	**p = 0.009**	n.s.	n.s.	day	3	0.1144

Table S5. a) Generalized-linear mixed effects model (GLMM) for the proportion of damaged leaves in the 2022 field experiment. Week, plant species, and their interaction were included as fixed effects. b) GLMM for the proportion of highly damaged leaves in the 2023 field experiment. Week, plant species, insecticide treatment, competition treatment, and all possible interactions were initially included as fixed effects. Because leaf damage was not recorded in week 9, interactions between competition treatment and week could not be fitted. A non-significant interaction of plant species × competition was removed from the full model, and statistics for the remaining terms are reported from the reduced model. An additive fixed effect of observer was included in all models.

a) Analysis of Deviance Table (Type III Wald Chisquare tests)

	Df	Chisq	p-value
Week	2	115.10	**< 0.001**
Plant	1	168.91	**< 0.001**
Week:Plant	2	54.17	**< 0.001**
Observer	3	92.11	**< 0.001**

Model: glmer(cbind(damaged,undamaged) ~ Week * Plant + Observer + (1|Plant ID) + (1| Genotype)

b) Analysis of Deviance Table (Type III Wald Chisquare tests)

	Df	Chisq	p-value
Week	2	65.64	**< 0.001**
Plant	1	126.52	**< 0.001**
Insecticide	1	0.55	0.457
Competition	1	8.09	**0.004**
Week:Plant	2	19.91	**< 0.001**
Week:Insecticide	2	39.06	**< 0.001**
Week:Plant:Insecticide	2	94.42	**< 0.001**
Plant:Insecticide	1	44.67	**< 0.001**
Plant:Competition	1	1.88	0.171
Insecticide:Competition	1	12.18	**< 0.004**
Observer	1	60.38	**< 0.001**

Model: glmer(cbind(highly damaged, low+undamaged) ~
Week * Plant * Insecticide + Competition + Plant:Competition + Insecticide:Competition
+ Observer + (1|Plant ID) + (1|Neighbour group) + (1|Genotype)

Table S6. Parameters of four-parameter logistic models of plant height growth. a) 2022 field experiment: Because plant height was only recorded three times, only two parameters could be estimated from the data. We therefore compared a series of models across biologically relevant ranges of t_{mid} and r for each species using AIC. After identifying optimal species-specific values for t_{mid} and r set, we refitted the full model to estimate H_0 and K using an *nlme* model. Reported parameters are either model estimates with 95% confidence intervals or fixed optimized values. The negative estimate of H_0 for *E. cheiranthoides* (implying negative height at transplanting) likely reflects limited data on early development. H_0, differed significantly by plant species, whereas there was no statistical support for plant-specific variation in K. b) 2023 field experiment: Weekly stem height measurements allowed the estimation of all four parameters using an *nlme* model. Reported parameters are model estimates with 95% confidence intervals. All parameters differed significantly between plant species, and K additionally varied with the plant species × insecticide interaction.

a) 2022 field experiment

	R. nigrum	*E. cheiranthoides*
H_0 (estimated)	19.56 [18.26 – 20.85]	-3.82 [-4.79 – -2.84]
K (estimated)	84.6 ± 1.91	
t_{mid} (fixed)	56	36
r (fixed)	0.10	0.09

b) 2023 field experiment

	R. nigrum		*E. cheiranthoides*	
	Ambient	Insecticide	Ambient	Insecticide
H_0 (estimated)	1.65 [1.29 – 2.01]		-0.23 [-0.39 – -0.08]	
K (estimated)	26.8 [18.3 – 35.3]	55.8 [46.9 – 64.8]	69.1 [66.0 – 72.1]	75.5 [72.4 – 78.6]
t_{mid} (estimated)	38.0 [35.8 – 40.2]		39.4 [38.6 – 40.1]	
r (estimated)	0.283 [0.230 – 0.369]		0.115 [0.111 – 0.118]	

Table S7. a) Linear mixed effects model (LMM) for ln-transformed biomass of plants in the 2022 field experiment, harvested in weeks 8, 11, and 14. Week, plant species, and their interaction were included as fixed effects. b) LMMs for ln-transformed biomass of plants in the 2023 field experiment, all harvested in week 10. Plant species, insecticide treatment, competition treatment, and all interactions were included as fixed effects.

a) Analysis of Deviance Table (Type III Wald Chisquare tests)

	Df	Chisq	p-value
Week	2	27.78	**< 0.001**
Plant	1	9.11	**0.003**
Week:Plant	2	6.49	**0.039**

Model: lmer(ln(biomass) ~ Week * Plant + (1| Genotype)

b) Analysis of Deviance Table (Type III Wald Chisquare tests)

	Df	Chisq	p-value
Plant	1	87.11	**< 0.001**
Insecticide	1	33.45	**< 0.001**
Competition	1	13.40	**< 0.001**
Plant:Insecticide	1	25.46	**< 0.001**
Plant:Competition	1	5.83	**0.016**
Insecticide:Competition	1	4.64	**0.031**
Plant:Insecticide:Competition	1	14.52	**< 0.001**

Model: lmer(ln(biomass) ~ Plant * Insecticide * Competition + (1|Genotype)

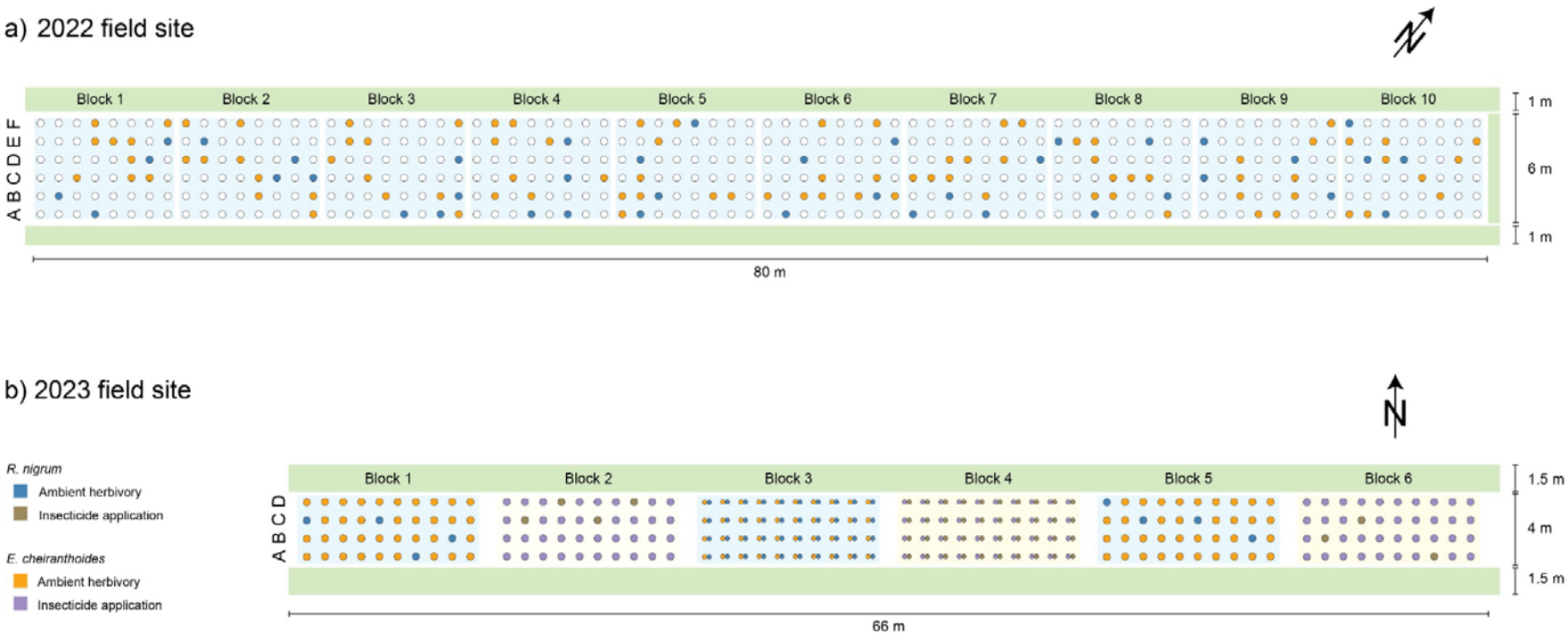

Figure S1. a) Schematic of the 2022 field site. Shown are the ten replicate blocks (light blue squares), with focal *R. nigrum* and *E. cheiranthoides* plants highlighted in colours. Empty circles are additional *E. cheiranthoides* plants belonging to genotypes not included for the analyses of this study. b) Schematic of the 2023 field site. Shown are the three blocks under ambient herbivory (light blue squares), and the three blocks receiving weekly applications of insecticide (light yellow squares). Paired circles in blocks 3 and 4 represent pairs of *R. nigrum* and *E. cheiranthoides* plants growing closely together in the same buried pot to impose plant-plant competition. Buffer strips sown with a mixture of *Raphanus sativus* and *Avena strigosa* are shown as light green rectangles for both years. Both sites were located adjacent to oilseed rape crop fields (not shown).

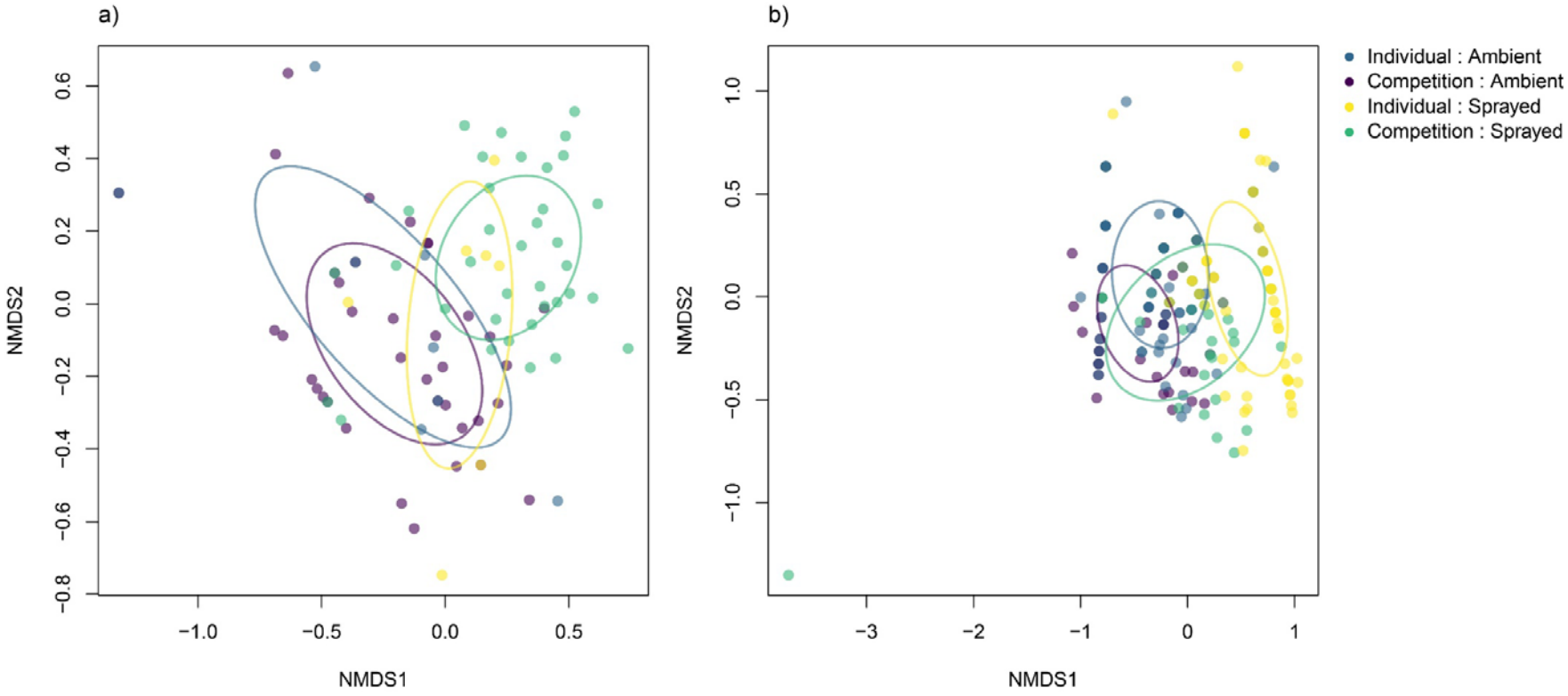

Figure S2. NMDS plots of the observed herbivore communities on a) *R. nigrum* or b) *E. cheiranthoides* in week 4 of the 2023 field experiment. Points are individual plants, with colours corresponding to the four combinations of the competition and insecticide treatment. Ellipses represent the within-treatment dispersion and show one standard deviation around the group centroid in NMDS space.

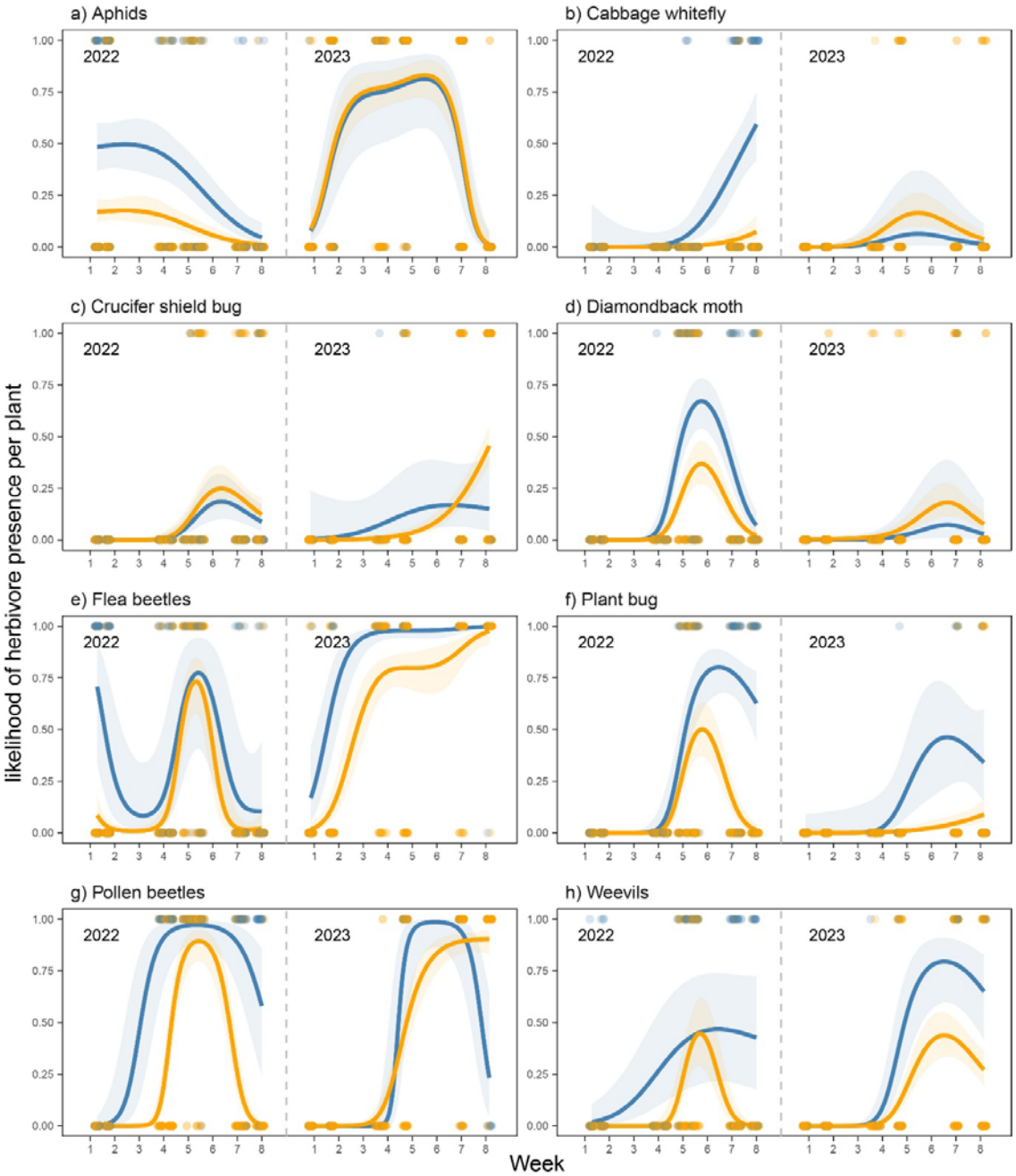

Figure S3. Likelihood of herbivore presence on *R. nigrum* (blue) and *E. cheiranthoides* (orange) in the 2022 and 2023 field experiment. Points are observations on individual plants, while lines and shaded are the mean model predictions and 95% confidence intervals from binomial generalized additive models (GAMs). All models used 'days in the field' as temporal variable, but the x-axes show 'week' for easier comparison with other results. See Supplementary Table S3 for test statistics of each model.

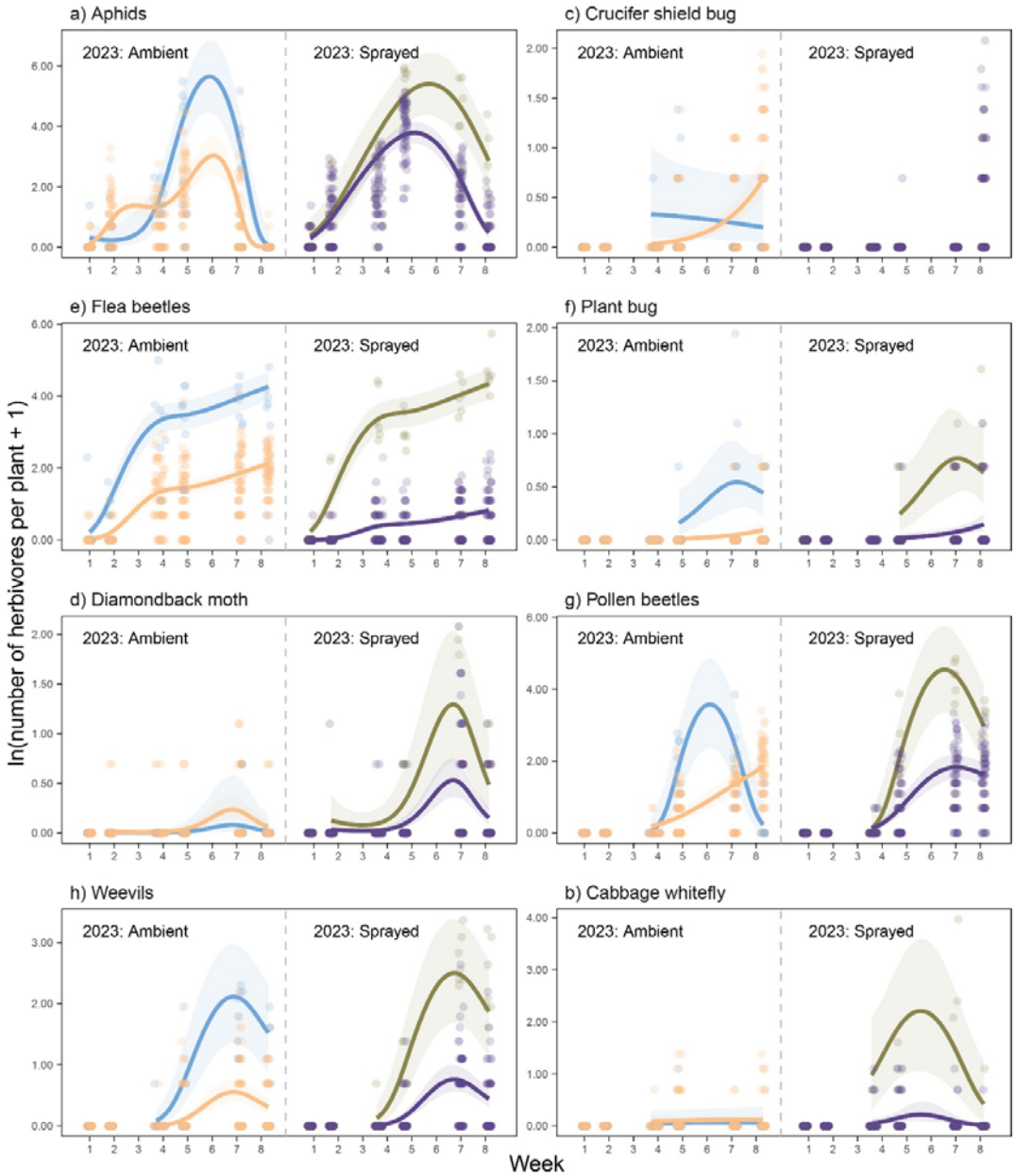

Figure S4. Herbivore abundance for the eight main herbivores under ambient or insecticide-treated conditions on individual *R. nigrum* (ambient = blue; sprayed = olive) or *E. cheiranthoides* (ambient = orange; sprayed = purple) plants in the 2023 field experiment. Points represent observations on individual plants, while lines and shaded show mean model predictions and 95% confidence intervals from negative binomial generalized additive models (GAMs). GAMs were fitted to count data after exclusion of weeks with zero observations. Each panel (a-h) shows treatment-specific predictions from the same model, which included insecticide as fixed effect. All models used 'days in the field' as temporal variable, but the x-axes show 'week' for easier comparison with other results. No model could be fit for crucifer shield bugs on insecticide-treated plants due to insufficient observations. See Supplementary Table S4 for test statistics of each model.

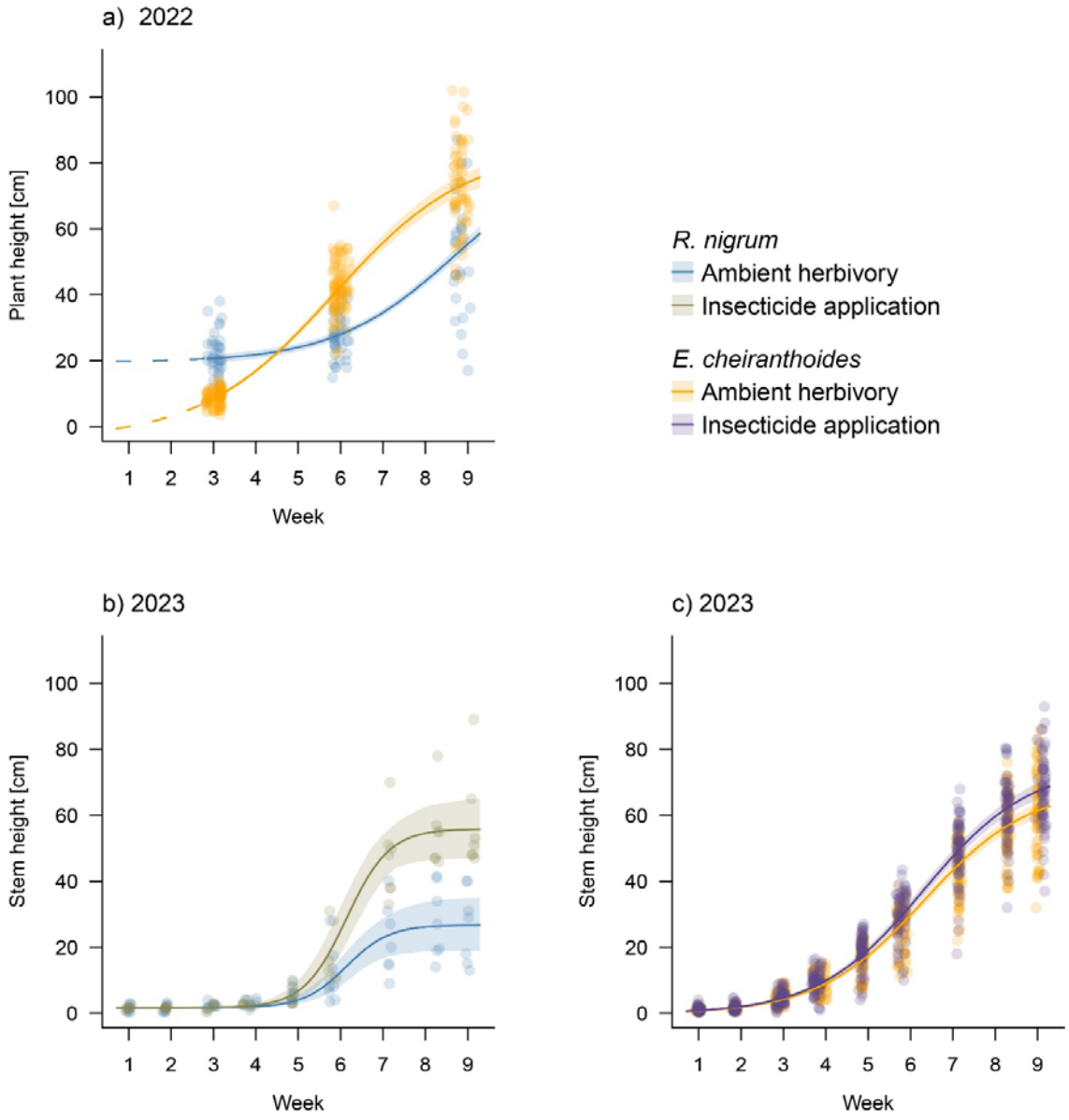

Figure S5. a) Plant height growth over nine weeks for *R. nigrum* and *E. cheiranthoides* in the 2022 field experiment. Points are individual plant measurements, and solid lines are model fits from a four-parameter logistic regression. Shaded areas indicate 95% confidence intervals (population prediction intervals). Plant height, measured from the root base to the tallest point of the plant, was first recorded in week 3; thus, the initial growth period (dashed lines) represents a backward extrapolation to the origin based on the fitted logistic function. b-c) Stem height growth for *R. nigrum* and *E. cheiranthoides* under ambient herbivory and insecticide treatment in the 2023 field experiment. Stem height was measured from the root base to the apical meristem of each plant, resulting in lower initial height values compared to 2022.

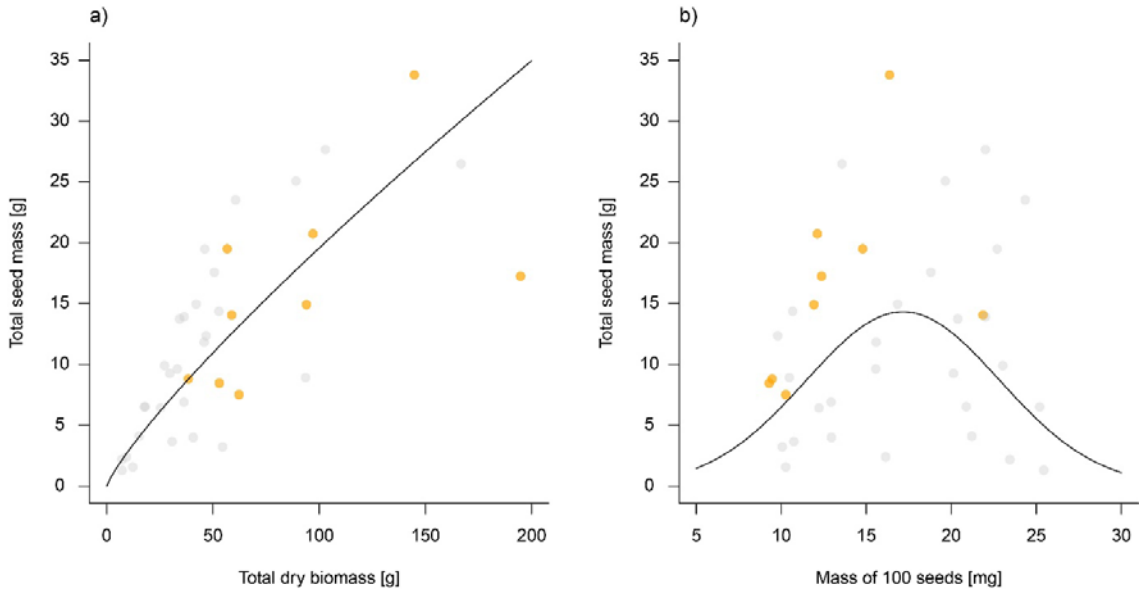

Figure S6. a) Relationship between total seed mass and aboveground plant biomass for *E. cheiranthoides* plants in the 2022 field experiment. Plants from block 7 were removed from the field intact and maintained in a greenhouse until seed ripening. Points represent individual plants, each corresponding to a different genotype. The solid line shows a linear fit between ln-transformed total seed mass and ln-transformed total biomass ($F_{1,36}$ = 77.48, p<0.001, R^2 = 0.67). Genotypes included in the main analyses are highlighted in orange, whereas excluded genotypes are shown grey. b) Relationship between total seed mass and individual seed mass. The solid line shows a quadratic fit between ln-transformed total seed mass and the mass of 100 seeds (quadratic term: $F_{1,35}$ = 7.15, p=0.011, R^2 = 0.12).

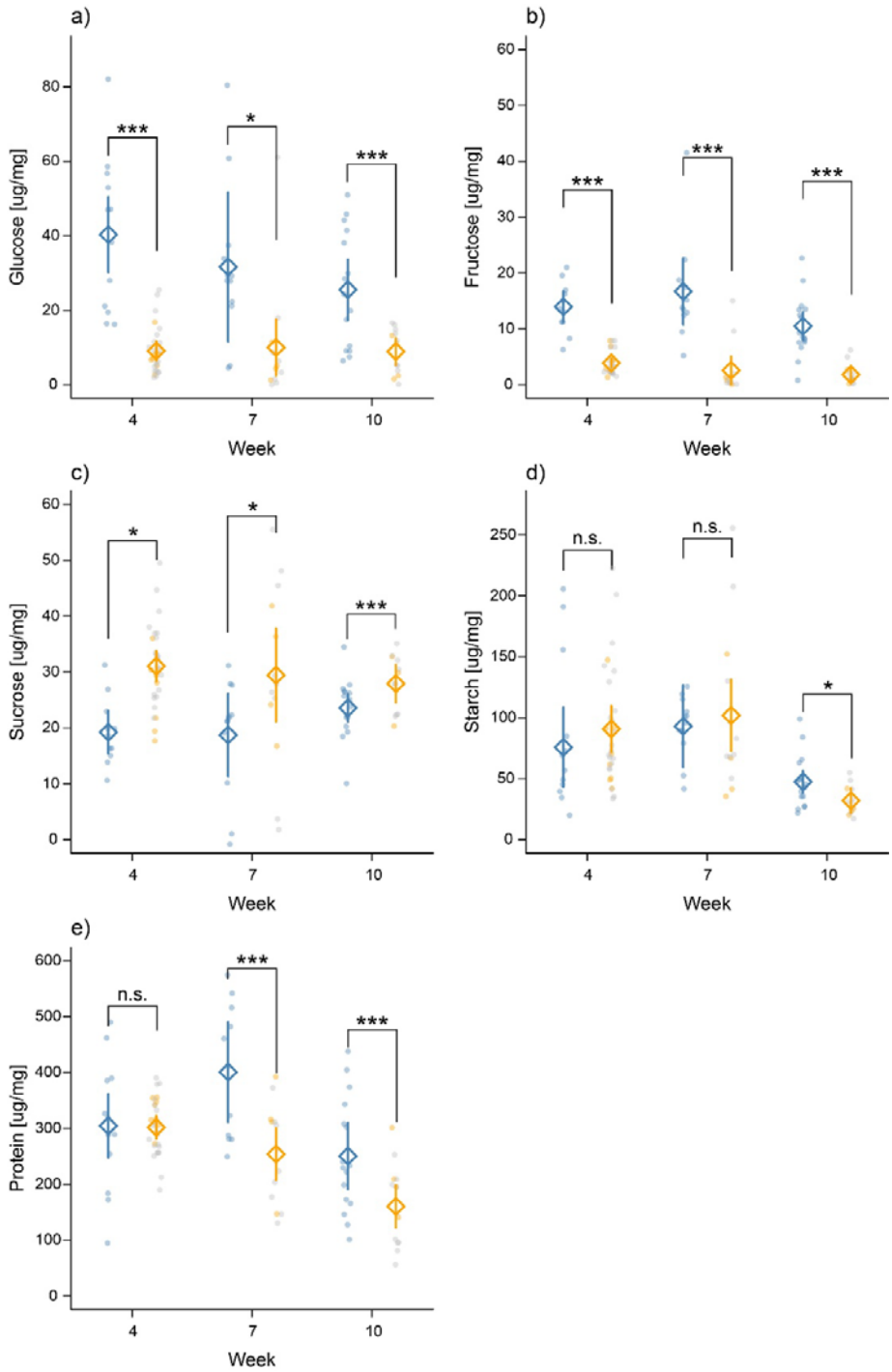

Figure S7. Concentrations of soluble sugars (a-c), starch (d), and total protein (d) in leaf tissue of *R. nigrum* (blue) and *E. cheiranthoides* (orange) harvested in weeks 4, 7, and 10 of the 2022 field experiment. Points are values for individual plants, while diamond symbols and lines are means and 95% confidence intervals from a linear model. Brackets highlight significant linear contrasts at the $p < 0.05$ level. For *E. cheiranthoides*, a random subset of plants from the full experiment was analysed, including genotypes excluded for other analyses in this study (grey points). Genotypes included in the main analyses are highlighted in orange, whereas excluded genotypes are shown grey.

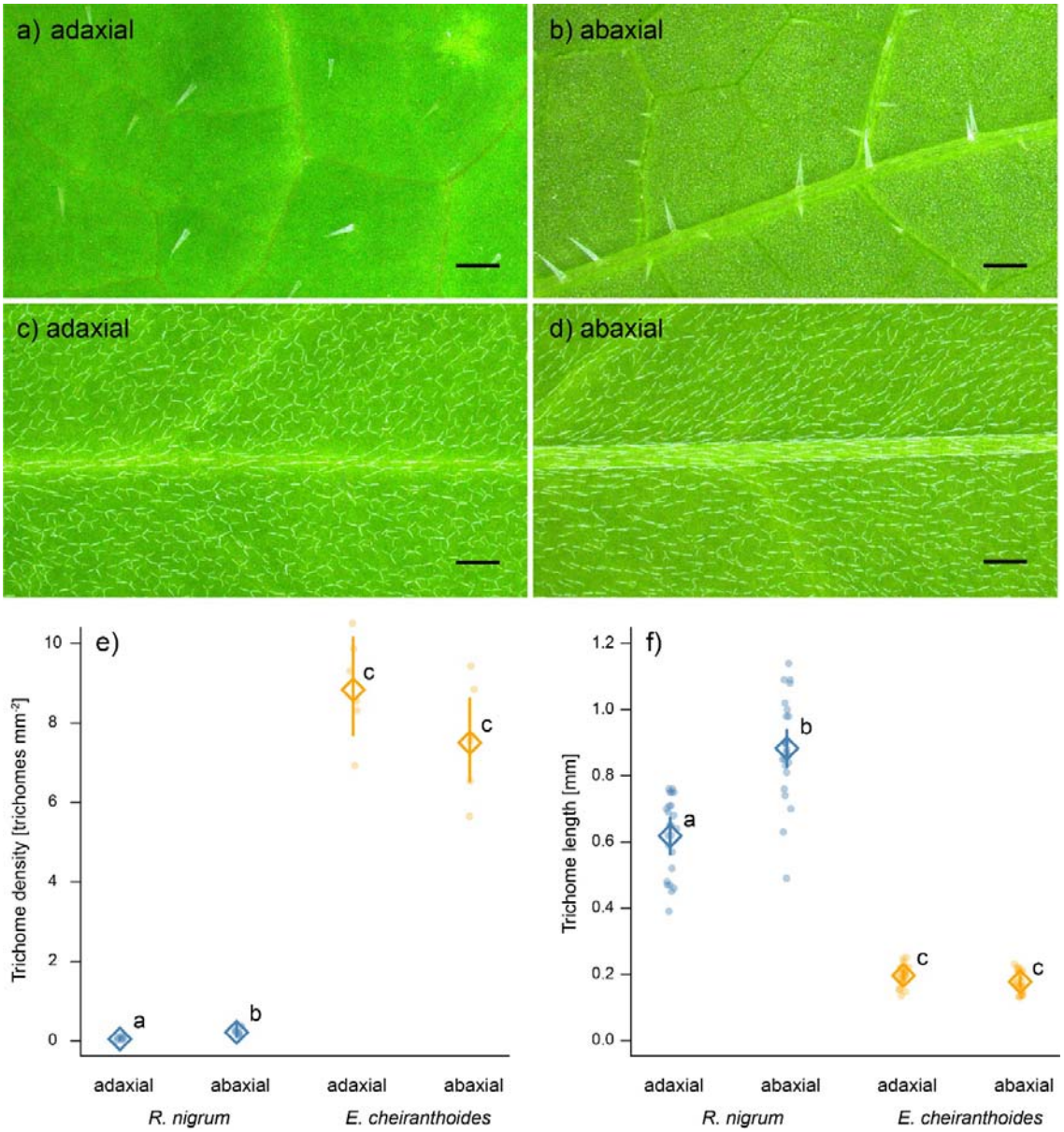

Figure S8. Photographs of the adaxial (upper) and abaxial (lower) leaf sides of 4-week-old *R. nigrum* (a-b) and *E. cheiranthoides* (c-d) plants growing under greenhouse conditions. Scale bars correspond to distances of 1 mm. Six photographs per side and species were used to quantify trichome densities (e) and trichome length (f). Points are values for individual plants, while diamonds and vertical lines are the means and 95% confidence intervals from linear models. Letters highlight significant linear contrasts at the $p < 0.05$ level.

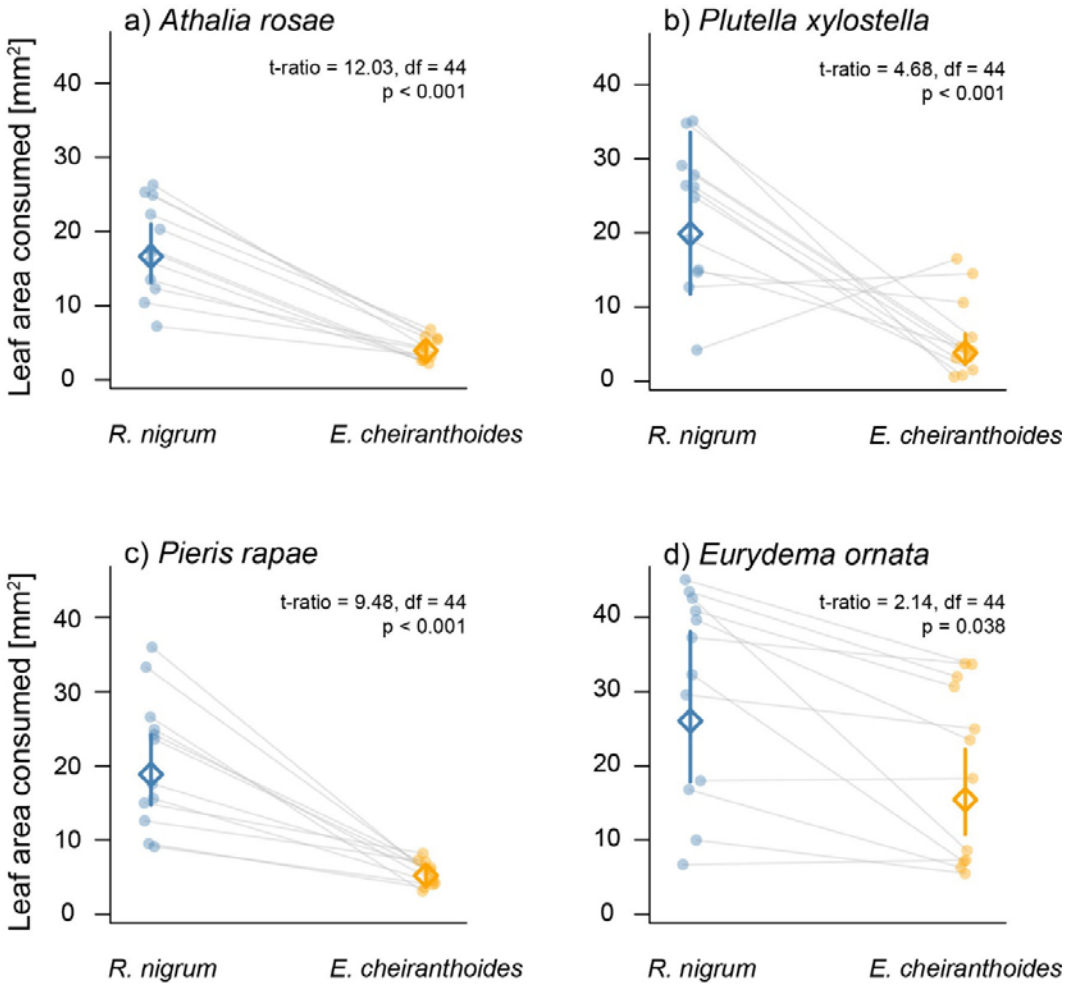

Figure S9. Relative preference of a) larvae of the turnip sawfly *Athalia rosae*, b) larvae of *P. xylostella*, c) larvae of the cabbage white butterfly *Pieris rapae*, or d), adult *E. ornata* in two-choice laboratory assays. Choice was quantified as leaf area eaten from pairs of leaf discs over 24 hours. Leaf discs (45 mm^2 area) came from 4-week-old *R. nigrum* and *E. cheiranthoides* plants grown under greenhouse conditions and were offered to herbivores in Petri dishes. Points are damage areas for individual leaf discs, with grey lines connecting pairs of leaf discs from the same dish. Diamonds and vertical lines are the means and 95% confidence from a linear mixed-effects model, while statistical tests are linear contrasts comparing consumption of the two plant species for each herbivore.